Reactivity, Structures, and NMR Spectroscopy of Half-Sandwich Pentamethylcyclopentadienyl Rhodium Amido Complexes Relevant to Transfer Hydrogenation

A. John Blacker,[†] Simon B. Duckett,[‡] Jake Grace,[‡] Robin N. Perutz,*[,‡] and Adrian C. Whitwood[‡]

Piramal Healthcare, Leeds Road, Huddersfield, U.K., HD1 9GA, and Department of Chemistry, University of York, York, U.K., YO10 5DD

Received October 15, 2008

The reactivity, structures, and NMR spectroscopy of a series of compounds relevant to asymmetric transfer hydrogenation, of general formula Cp*RhCl(*S,S*-4-$RC_6H_4SO_2NCHPhCHPhNH_2$) (Cp* = η^5-C_5Me_5, *S,S*-**2a** R = Me, *S,S*-**2b** R = *t*Bu, *S,S*-**2c** R = F), have been studied. $^1H/^{15}N$ HMQC NMR spectra of **2a**−**2c** were recorded with ^{15}N in natural abundance making use of the coupling to the C_5Me_5 protons; the coupling constants J_{RhN} were ca. 15 and 20 Hz for the amino and amido nitrogens, respectively. $^1H/^{103}Rh$ NMR spectra of **2a** and **2c** were recorded similarly. The chloride ligand in *S,S*-**2a** has been shown to be very labile; reaction with CO afforded the cationic complex [Cp*Rh(CO){C(O)N-(Ts)CHPhCHPhNH$_2$}][Cl] (**3a**) as a mixture of diastereomers, S,S,R_{Rh} and S,S,S_{Rh}, with opposite chirality at Rh; reaction with *t*BuNC gave [Cp*Rh(CN*t*Bu)(*S,S*-TsCHPhCHPhNH$_2$)][PF_6] (**4a**), and reactions with LiBr and KI gave Cp*RhBr(*S,S*-TsNCHPhCHPhNH$_2$) (**6a**) and Cp*RhI(*S,S*-TsNCHPhCHPhNH$_2$) (**7a**), respectively. Complexes *S*,*S*-**2c**, *S*,*S*-**6a**, and *S*,*S*-**7a** have been characterized by X-ray crystallography; the amino N−Rh bond is significantly shorter than the amido N−Rh bond in all cases (difference Δr 0.058(2), 0.085(6), and 0.046(4) Å, respectively), and the complexes all possess intramolecular NH···X (X = Cl, Br, I) hydrogen bonds. The reaction of **2a** with formic acid results in complete displacement of the chelating ligand and the formation of dinuclear [{Cp*Rh}$_2$(μ-H)(μ-Cl)(μ-HCO_2)][BPh_4] (**5a**), which was also characterized crystallographically. Reaction of **2c** with AgOTf resulted in the formation of [Cp*Rh(OH_2)(4-$FC_6H_4SO_2NCHPhCHPhNH_2$)][OTf] (**[8c·H$_2$O][OTf]**) or [Cp*Rh(4-$FC_6H_4SO_2NCHPhCHPhNH_2$)]$_2$-[OTf]$_2$ (**[8c]$_2$[OTf]$_2$**) depending upon the conditions employed. **[8c·H$_2$O][OTf]** was characterized by X-ray crystallography, and the structure showed that both CHPh centers in the ligand had been racemized, converting the *S,S* isomer of the starting material into a mixture of both *R,R* and *S,S* isomers.

Introduction

Asymmetric transfer hydrogenation catalyzed by half-sandwich complexes with monotosylated diamine ligands was described first by Noyori et al.[1,2] The mechanism for the transfer hydrogenation of CO double bonds with *i*PrOH/KOH as the hydrogen donor has been described as outer-sphere metal−ligand bifunctional catalysis;[3] a schematic for the [(*p*-cymene)$RuCl_2$]$_2$/TsDPEN (TsDPEN = *N*-tosyl 1,2-diphenylethylenediamine) system is shown in Figure 1. First, [(*p*-cymene)$RuCl_2$]$_2$ and TsDPEN react to form the catalyst precursor (step 1). The precursor then reacts with base (KOH) to give a 16-electron species (step 2), which is hydrogenated by *i*PrOH (the hydrogen donor), leading to an 18-electron hydride complex (step 3). The latter transfers its hydride to the carbonyl carbon of the substrate and a proton from its amino nitrogen to the oxygen of the substrate, to give the product alcohol and re-form the 16-electron species (step 4). Step 4 is proposed to transfer hydrogen via a six-membered, pericyclic transition state, without coordination of the substrate to Ru.

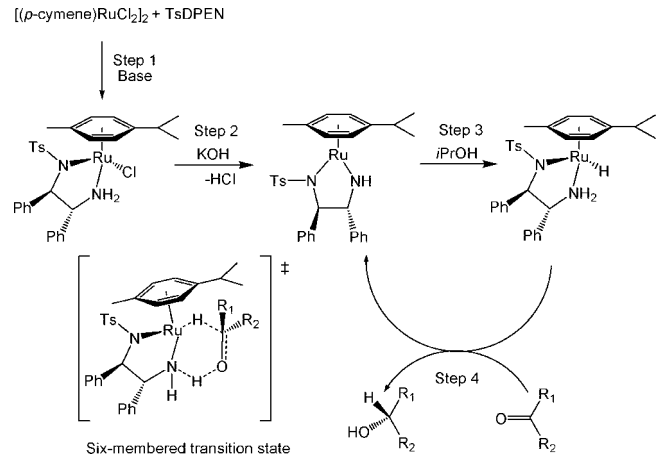

Figure 1. Proposed catalytic cycle for outer-sphere metal−ligand bifunctional catalysis.[3]

Catalytic transfer hydrogenation of C=N bonds using HCO_2H and its salts as the hydrogen donor[4−12] was first reported by Noyori and co-workers in 1996.[4,13] Due to its operational simplicity and wide substrate scope, it has become the method of choice for the synthesis of many chiral amines.

* Corresponding author. E-mail: rnp1@york.ac.uk.
[†] Piramal Healthcare.
[‡] University of York.

(1) Hashiguchi, S.; Fujii, A.; Takehara, J.; Ikariya, T.; Noyori, R. *J. Am. Chem. Soc.* **1995**, *117*, 7562.
(2) Noyori, R.; Hashiguchi, S. *Acc. Chem. Res.* **1997**, *30*, 97.
(3) Haack, K. J.; Hashiguchi, S.; Fujii, A.; Ikariya, T.; Noyori, R. *Angew. Chem., Int. Ed.* **1997**, *36*, 285.

10.1021/om8009969 CCC: $40.75
Publication on Web 02/09/2009

Noyori and co-workers have isolated and characterized all three ruthenium complexes in Figure 1 by X-ray crystallography and have shown that they all reduce acetophenone with comparable activity and selectivity.[3] Following this, attempts were made to study the behavior of the analogous Cp*M(III) (M = Rh or Ir, Cp* = η^5-C_5Me_5) systems;[14−17] however, these systems are generally more active and the analogous intermediates have proved harder to isolate (the rhodium and iridium systems are also described in patents belonging to Piramal Healthcare).[18−20] Tani et al. showed that $[Cp^*RhCl_2]_2$ and TsDPEN react with NaOH to give the 16-electron species Cp*Rh(TsNCHPhCHPhNH),[14] but the rhodium hydride complex proved elusive. For iridium, a bis-amido 16-electron species was obtained as described above for rhodium; the same product was obtained by reaction of the chloride precursor with aqueous KOH in CH_2Cl_2. The hydride Cp*Ir(H)(TsNCHPhCHPhNH$_2$) was then prepared by reaction of this 16-electron complex with *i*PrOH. The reverse reaction of the hydride complex with acetone gave back the bis-amido complex.[14]

Ikariya and co-workers reported the synthesis of the related complexes Cp*RhCl(TsNC$_6$H$_{10}$NH$_2$) (where C$_6$H$_{10}$ is 1,2-disubstituted cyclohexane), Cp*RhCl(TsNCHPhCHPhNH$_2$), Cp*IrCl(TsNC$_6$H$_{10}$NH$_2$), and Cp*IrCl(TsNCHPhCHPhNH$_2$), which also act as catalyst precursors for the asymmetric transfer hydrogenation of acetophenones.[15,16] They showed that the reaction of Cp*IrCl(TsNC$_6$H$_{10}$NH$_2$) with 1 equiv of NaOH in *i*PrOH gave quantitative conversion to the 18-electron hydride Cp*Ir(H)(TsNC$_6$H$_{10}$NH$_2$), which then reacted with acetone to give the bis-amido complex Cp*Ir(TsNC$_6$H$_{10}$NH). Recently, Heiden and Rauchfuss exploited the interconversion of Cp*Ir(TsNCHPhCHPhNH), $[Cp^*Ir(TsNCHPhCHPhNH_2)]^+$, and Cp*Ir(H)(TsNCHPhCHPhNH$_2$), to demonstrate that the hydride complex acts as a catalyst for the conversion of dihydrogen and dioxygen to water.[21] They also showed that the 16-electron cation $[Cp^*Ir(TsNCHPhCHPhNH_2)]^+$ reacts with Lewis bases to form simple adducts $[Cp^*Ir(TsNCHPhCHPhNH_2)L]^+$ (L = MeCN, NH_3, PAr_3, and CO).[22]

In spite of the successful synthesis of these 16-electron and hydride species, there has still been considerable debate about their role in the transfer hydrogenation of imines. Evidence from isotope labeling supports a monohydride mechanism in which the hydride and the proton undergoing transfer remain distinct for Rh, Ir, and Ru catalysts.[23−25] On the other hand, it has been much harder to define when the outer-sphere (Noyori mechanism) occurs and when a more conventional inner-sphere mechanism occurs in which the substrate binds directly to the metal.[11,26−33]

A better understanding of the chemistry of complexes such as Cp*RhCl(TsNCHPhCHPhNH$_2$) (**2a**) will surely aid our understanding of the catalytic systems, since **2a** is generated *in situ* in catalytic asymmetric transfer hydrogenation reactions (the process is named CATHy, catalytic asymmetric transfer hydrogenation).[18−20] It also catalyzes the asymmetric Michael addition reaction[34,35] and reacts with sodium phenoxide in dichloromethane, albeit very slowly and in low yield, to give a cyclometalated product.[36]

Our aim was to study the reactivity of the catalyst **2a** with a focus on the identification of complexes relevant to transfer hydrogenation. Because of the poor solubility of the complexes derived from *N*-tosyl-1,2-diphenylethylenediamine (TsDPEN) (**1a**), we synthesized two additional ligand precursors, 4-*t*Bu-C$_6$H$_4$SO$_2$DPEN) (**1b**) and 4-FC$_6$H$_4$SO$_2$DPEN (**1c**). The resulting metal complexes were more soluble than those of **1a**, and the F atom in **1c** provided an additional NMR handle. We describe the reactions with CO, *t*BuNC, and AgOTf leading to cationic complexes. We show that the reaction of **2a** with HCO_2H displaces the chelating chiral ligand completely. We also include the metathesis reactions that allow replacement of chloride with bromide and iodide. Throughout this work, we place emphasis on structural features including intramolecular hydrogen bonding (as noted previously)[3,5,15] that we investigate through X-ray crystallography and NMR spectroscopy. We have also recorded ^{15}N and ^{103}Rh NMR spectra as additional probes.

Results and Discussion

Synthesis and Structure of Cp*RhCl(4-RC$_6$H$_4$SO$_2$NCHPhCHPhNH$_2$), 2a−2c. The N-aromatic sulfonyl-1,2-diphenylethylenediamine ligands were synthesized by the method of White et al. (Scheme 1).[37] Both the *R,R* and *S,S* isomers of **1b** and **1c** were prepared, but we show the *S,S* isomers in the schemes.

The ligands **1a**−**1c** were complexed to rhodium by reaction with $[Cp^*RhCl_2]_2$ to yield Cp*RhCl(4-RC$_6$H$_4$SO$_2$NCHPhCHPhNH$_2$) [**2a** (R = Me), **2b** (R = *t*Bu), and **2c** (R = F)]. Complex

(4) Hashiguchi, S.; Uematsu, N.; Noyori, R. *J. Synth. Org. Chem. Jpn.* **1997**, *55*, 99.
(5) Mao, J. M.; Baker, D. C. *Org. Lett.* **1999**, *1*, 841.
(6) Chrzanowska, M.; Rozwadowska, M. D. *Chem. Rev.* **2004**, *104*, 3341.
(7) Vedejs, E.; Trapencieris, P.; Suna, E. *J. Org. Chem.* **1999**, *64*, 6724.
(8) Meuzelaar, G. J.; van Vliet, M. C. A.; Maat, L.; Sheldon, R. A. *Eur. J. Org. Chem.* **1999**, 2315.
(9) Kaldor, I.; Feldman, P. L.; Mook, R. A.; Ray, J. A.; Samano, V.; Sefler, A. M.; Thompson, J. B.; Travis, B. R.; Boros, E. E. *J. Org. Chem.* **2001**, *66*, 3495.
(10) Roszkowski, P.; Wojtasiewicz, K.; Leniewski, A.; Maurin, J. K.; Lis, T.; Czarnocki, Z. *J. Mol. Catal. A: Chem.* **2005**, *232*, 143.
(11) Samec, J. S. M.; Bäckvall, J.-E.; Andersson, P. G.; Brandt, P. *Chem. Soc. Rev.* **2006**, *35*, 237.
(12) Clapham, S. E.; Hadzovic, A.; Morris, R. H. *Coord. Chem. Rev.* **2004**, *248*, 2201.
(13) Uematsu, N.; Fujii, A.; Hashiguchi, S.; Ikariya, T.; Noyori, R. *J. Am. Chem. Soc.* **1996**, *118*, 4916.
(14) Mashima, K.; Abe, T.; Tani, K. *Chem. Lett.* **1998**, 1201.
(15) Murata, K.; Ikariya, T.; Noyori, R. *J. Org. Chem.* **1999**, *64*, 2186.
(16) Ikariya, T.; Blacker, A. J. *Acc. Chem. Res.* **2007**, *40*, 1300.
(17) Mashima, K.; Abe, T.; Tani, K. *Chem. Lett.* **1998**, 1199.
(18) Blacker, A. J. *Handbook of Homogeneous Hydrogenation*; Wiley-VCH:: New York, 2007.
(19) Blacker, A. J.; Mellor, B. EP971865B1, 1997.
(20) Blacker, A. J.; Martin, J. Scale up Studies in Asymmetric Transfer Hydrogenation. In *Asymmetric Catalysis on Industrial Scale*; Blaser, H.-U.; Schmidt, E., Eds.; Wiley-VCH: Weinheim, 2004; p 201.
(21) Heiden, Z. M.; Rauchfuss, T. B. *J. Am. Chem. Soc.* **2007**, *129*, 14303.
(22) Heiden, Z. M.; Gorecki, B. J.; Rauchfuss, T. B. *Organometallics* **2008**, *27*, 1542.
(23) Samec, J. S. M.; Ell, A. H.; Åberg, J. B.; Privalov, T.; Eriksson, L.; Bäckvall, J.-E. *J. Am. Chem. Soc.* **2006**, *128*, 14293.
(24) Casey, C. P.; Singer, S. W.; Powell, D. R.; Hayashi, R. K.; Kavana, M. *J. Am. Chem. Soc.* **2001**, *123*, 1090.
(25) Casey, C. P.; Johnson, J. B. *J. Org. Chem.* **2003**, *68*, 1998.
(26) Samec, J. S. M.; Ell, A. H.; Bäckvall, J.-E. *Chem. Commun.* **2004**, 2478.
(27) Ell, A. H.; Johnson, J. B.; Bäckvall, J.-E. *Chem. Commun.* **2003**, 1652.
(28) Casey, C. P.; Johnson, J. B. *J. Am. Chem. Soc.* **2005**, *127*, 1883.
(29) Casey, C. P.; Beetner, S. E.; Johnson, J. B. *J. Am. Chem. Soc.* **2008**, *130*, 2285.
(30) Privalov, T.; Samec, J. S. M.; Bäckvall, J.-E. *Organometallics* **2007**, *26*, 2840.
(31) Johnson, J. B.; Bäckvall, J.-E. *J. Org. Chem.* **2003**, *68*, 7681.
(32) Casey, C. P.; Bikzhanova, G. A.; Cui, Q.; Guzei, I. A. *J. Am. Chem. Soc.* **2005**, *127*, 14062.
(33) Casey, C. P.; Johnson, J. B.; Singer, S. W.; Cui, Q. *J. Am. Chem. Soc.* **2005**, *127*, 3100.
(34) Watanabe, M.; Murata, K.; Ikariya, T. *J. Am. Chem. Soc.* **2003**, *125*, 7508.

Scheme 1. Synthesis of 1a−1c

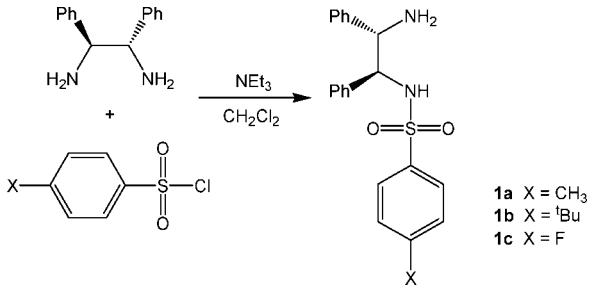

2a has been described previously.[5,15,17,19] Complexes **2a**−**2c** were prepared by treatment of $[Cp^*RhCl_2]_2$ with **1a**−**1c** and NEt_3 in CH_2Cl_2 and were crystallized as red-orange needles. The most interesting features of the ^1H NMR spectra of **2a**−**2c** are the chemical shift changes for the NH_2 protons that were observed when the solvent was changed. For **2a**, the NH protons are observed at δ 3.46 and 3.88 in CD_2Cl_2, but are shifted to δ 4.42 and 3.60 in CD_3CN (Figure 2). This is consistent with intramolecular hydrogen bonding in CD_2Cl_2, a weak H-bond acceptor, and a more important role for intermolecular hydrogen bonding in CD_3CN, a stronger hydrogen bond acceptor. The acidity of the NH protons was confirmed when exchange with deuterium was observed in CD_3OD (Figure 2). The coupling constants of the C*H*Ph-C*H*Ph protons (H^5 and H^{10}), at 11−12 Hz, are diagnostic of three-bond couplings between diaxial, vicinal protons.[38−40] This feature indicates that the phenyl groups are equatorial in the five-membered Rh−N−C−C−N ring, in agreement with the X-ray structure (see below).

Complex *S,S*-**2c** was characterized by X-ray crystal analysis (Figure 3). Table 1 compares its structure to those of **2a**,[5] the related ruthenium complex, [(*p*-cymene)RuCl(TsNCHPhCHPhNH$_2$)],[3] and bromide and iodide analogues described below. The amine hydrogen atoms were located in a difference map and refined isotropically, thereby demonstrating the presence of the intramolecular NH···Cl hydrogen bond. Further discussion of the structure is postponed until the other halide complexes have been described.

It has recently been suggested that [(arene)Ru(monotosylamidoamine)] complexes form dimers in solution through hydrogen bonding between the NH protons of one molecule and a sulfonyl oxygen of another, or between the NH protons of one molecule and the chloride of a second.[41] This has been demonstrated by PGSE NMR experiments and calculations, and also by ESI mass spectrometry. An ESI mass spectrum of **2a** (in CH_3OH) showed a peak at m/z = 603 for the monomer $[M - Cl]^+$ and also at m/z = 1241 for $[M_2 - Cl]^+$, suggesting that both monomer and dimer may be present in solution.

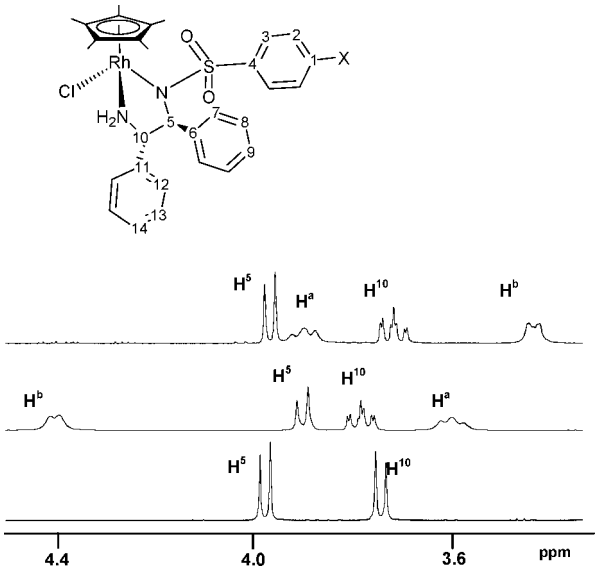

Figure 2. ^1H NMR spectra of **2a** in CD_2Cl_2 (top), CD_3CN (middle), and CD_3OD (bottom).

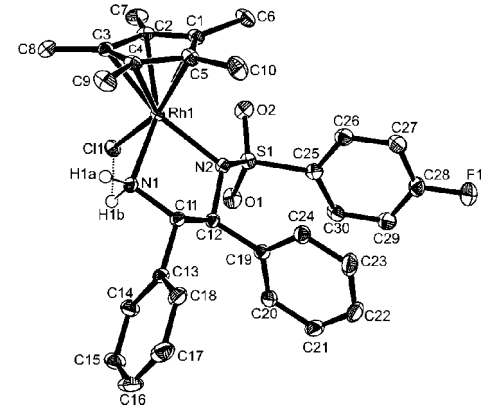

Figure 3. Molecular structure of *S,S*-**2c** (thermal ellipsoids shown at 50% probability). Hydrogen atoms are omitted except for those of the amino group. The dotted line shows the hydrogen bond.

Table 1. Selected Bond Lengths (Å) and Angles (deg) for 2a, 2c, 6a, 7a, and Ru

	complex				
bond	**2a**[a] (X = Cl)	**2c** (X = Cl)	**6a** (X = Br)	**7a** (X = I)	**Ru**[b] (X = Cl)
M−X	2.421(5)	2.4175(5)	2.4968(7)	2.7107(3)	2.435(4)
M−N(1)	2.103(6)	2.1069(17)	2.101(4)	2.122(3)	2.116(9)
M−N(2)	2.184(6)	2.1649(17)	2.186(4)	2.168(2)	2.145(8)
Δr(M−N)[d]	0.081(8)	0.058(2)	0.085(6)	0.046(4)	0.029(12)
N(1)−M−N(2)	77.5(5)	78.70(6)	77.27(15)	78.76(10)	79.5(3)
N(1)−M−X	84.1(2)	83.36(5)	84.52(12)	84.01(8)	81.1(2)
N(2)−M−X	94.0(2)	91.81(5)	94.65(10)	93.75(6)	86.4(2)
X···N(1)	3.032(7)	3.0183(19)	3.106(4)	3.263(3)	2.968(10)
X···HN(1)		2.55(2)	2.61[c]	2.78(3)	2.57[c]
X···H−N(1)		111.7(17)	123[c]	115(2)	104[c]

[a] Ref 5, H not located. [b] Ref 3 **Ru** = [(*p*-cymene)RuCl(TsNCHPhCHPhNH$_2$)]. [c] No esd available since hydrogen location could not be refined, or was not refined. [d] Δr(M−N) is the difference between the two Rh−N distances.

We also wished to determine ^{15}N NMR data for **2a** as a basis for further study of catalytic intermediates. [^{15}N]-TsDPEN was synthesized as a mixture of *R,R* and *S,S* isomers according to the method of Corey et al. (Scheme 2) with ca. 40% ^{15}N.[42] It was not necessary to resolve the racemic mixture because the ^1H NMR spectra of the associated metal complexes are identical. The DPEN ligand was tosylated to give ^{15}N-labeled TsDPEN (**1a-^{15}N**) in 46% yield. The FAB mass spectrum for **1a-^{15}N**

(35) Watanabe, M.; Ikagawa, A.; Wang, H.; Murata, K.; Ikariya, T. *J. Am. Chem. Soc.* **2004**, *126*, 11148.
(36) Koike, T.; Ikariya, T. *Organometallics* **2005**, *24*, 724.
(37) Soleimannejad, J.; Sisson, A.; White, C. *Inorg. Chim. Acta* **2003**, *352*, 121.
(38) Tormena, C. F.; Vilcachagua, J. D.; Karcher, V.; Rittner, R.; Contreras, R. H. *Magn. Reson. Chem.* **2007**, *45*, 590.
(39) Sudmeier, J. L.; Blackmer, G. L. *Inorg. Chem.* **1971**, *10*, 2010.
(40) Pouzard, G.; Rajzmann, M.; Bodot, H.; Pujol, L. *Org. Magn. Reson.* **1973**, *5*, 209.
(41) Pelagatti, P.; Carcelli, M.; Calbiani, F.; Cassi, C.; Elviri, L.; Pelizzi, C.; Rizzotti, U.; Rogolino, D. *Organometallics* **2005**, *24*, 5836.

Scheme 2. Synthesis of [^{15}N]-DPEN[a]

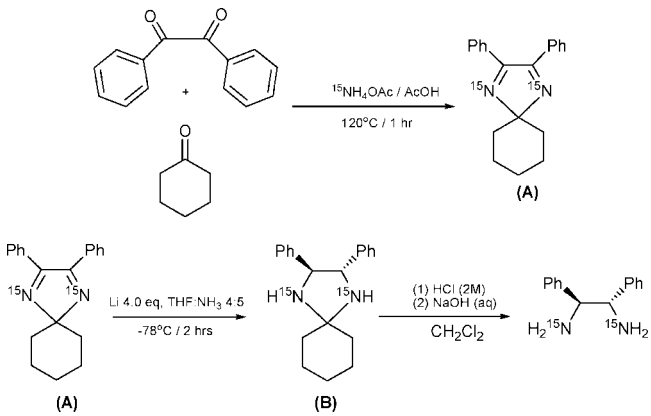

[a] 40% ^{15}N-labeled NH_4OAc was used, and a full range of isotopomers were formed; only the *S,S* isomer is shown but a mixture of *S,S* and *R,R* isomers was formed.

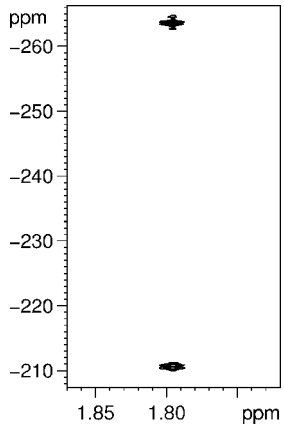

Figure 4. ^{1}H−^{15}N HMQC spectrum of **2a-^{15}N** (CD_2Cl_2, 300 K) showing couplings between the two nitrogen nuclei and the C_5Me_5 protons. $\delta(^{1}H)$ horizontal, $\delta(^{15}N)$ vertical.

compared well with the calculated spectrum. ^{15}N-Labeled **2a** (designated **2a-^{15}N**) was synthesized from **1a-^{15}N**, as described above.

The ^{1}H NMR spectrum (500 MHz, CD_2Cl_2, 300K) of **2a-^{15}N** displays coupling of both NH protons to ^{15}N. In the ^{15}N-enriched complex, H^a (numbering in Figure 2) generates two apparent triplet resonances with $J_{NH} = 82$ Hz on either side of the peak of the ^{14}N isotopomer. Proton H^b generates two doublets with $J_{NH} = 72$ Hz on either side of the doublet of the ^{14}N isotopomer. A ^{1}H−^{15}N HMQC spectrum showed a multiplet at δ −263.6 assigned as the amino nitrogen with coupling to both NH protons, H^5, H^{10}, and the $C_5(CH_3)_5$ protons. A second multiplet at δ −210.6 with coupling to H^5, H^{10}, and the $C_5(CH_3)_5$ protons was assigned as the amido nitrogen. A ^{1}H–^{15}N HMQC spectrum (50.7 MHz, CD_2Cl_2, 300 K) was recorded and showed Rh coupled doublets at δ −263.6 and −210.6 with $J_{RhN} = 14$ and 18 Hz, respectively (Figure 4). The observation of coupling between the TsDPEN ligand nitrogens and the protons of the Cp* ligand led us to try recording natural abundance ^{1}H/^{15}N HMQC spectra of complexes **2a**−**2c**. This was found to be surprisingly straightforward. Complex **2b** had peaks at δ −263.7 and −209.5 with $J_{RhN} = 17$ and 20 Hz, respectively, while complex **2c** showed ^{15}N peaks at δ −263.8 and −210.2 with $J_{RhN} = 16$ and 21 Hz, respectively.

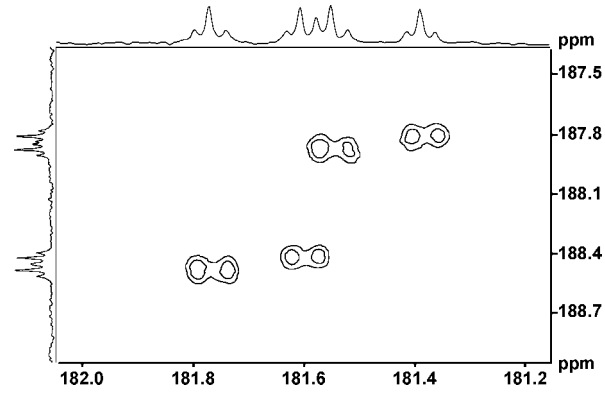

Figure 5. ^{13}C−^{13}C COSY (125 MHz, CD_2Cl_2, 300 K) experiment, showing couplings between the terminal CO and acyl CO in the two diastereomers of ^{13}C-labeled **3a**.

^{103}Rh NMR chemical shifts were also recorded via a ^{1}H−^{103}Rh HMQC method making use of the coupling to the C_5Me_5 protons (data in Experimental Section).

Reactivity of Cp*RhCl(TsNCHPhCHPhNH$_2$), 2a−2c. 1. Reactions with Carbon Monoxide, *tert*-Butylisonitrile, and Formic Acid. Rhodium complexes are known to catalyze both the decomposition of HCO_2H[43] and the water-gas shift reaction,[44] thereby providing a potential source of CO. The reactivity of the catalytic species toward CO is therefore of interest when using HCO_2H for transfer hydrogenation. CO (3 atm) was admitted to a solution of *S,S*-**2a** in CD_2Cl_2, and the reaction was followed by ^{1}H NMR spectroscopy. Over a period of 5 days, the Cp* resonance of *S,S*-**2a** at δ 1.80 decreased in intensity and was replaced by two new Cp* proton signals at δ 1.68 and 1.83 with approximately equal intensities, indicating complete conversion to products. Over an extended period, the system evolves further and $Cp^*Rh(CO)_2$ is formed as the major product, as indicated by the associated ^{1}H and ^{13}C NMR spectra and IR spectrum. Analysis of the first stage of reaction suggested that the initial products were two diastereoisomers *S,S,*R_{Rh} and *S,S,*S_{Rh} of [Cp*Rh(CO){C(O)N(Ts)CHPhCHPhNH$_2$}][Cl] (**3a**) with the same ligand chirality, but with opposite chirality at Rh. The ^{13}C NMR spectrum of the two diastereomers of **3a** shows resonances at δ 181.6 (d, $J_{RhC} = 27$ Hz) and 181.7 (d, $J_{RhC} = 27$ Hz) assigned to OCN and signals at δ 188.1 (d, $J_{RhC} = 77$ Hz) and 188.2 (d, $J_{RhC} = 77$ Hz) for the CO ligands. A ^{13}C−^{13}C COSY spectrum of **3a** (synthesized by reaction of **2a** with 1 atm ^{13}CO and 2 atm ^{12}CO) showed couplings between RhCO at 188.1 and the OCN at δ 181.6, along with couplings between the CO at δ 188.2 and the OCN at δ 181.7 (Figure 5), consistent with the presence of two diastereomers. The ^{1}H NMR spectrum (500 MHz, CD_2Cl_2, 300 K) of **3a** showed two peaks for Cp* (δ 1.68 and 1.83), two for the tosyl methyl group (δ 2.28 and 2.31), for the CH protons of the backbone, and for the NH protons. All these observations are consistent with the formation of a pair of diastereoisomers.

Complex **3a** may form via substitution of chloride by CO, followed by migration of the amide bond of the chelating ligand onto CO, which creates a coordinatively unsaturated, planar, 16-electron, carbamoyl complex. CO could then bind from the front or the back, forming two diastereomers of **3a** with the same ligand chirality, but with opposite chirality at Rh (Scheme

(42) Corey, E. J.; Imwinkelried, R.; Pikul, S.; Xiang, Y. B. *J. Am. Chem. Soc.* **1989**, *111*, 5493.

(43) King, R. B.; Bhattachayya, N. K. *Inorg. Chim. Acta* **1995**, *237*, 65.

(44) Cheng, C. H.; Hendriksen, D. E.; Eisenberg, R. *J. Am. Chem. Soc.* **1977**, *99*, 2791.

Scheme 3. Proposed Mechanism for the Reaction of 2a with CO to Form 5a

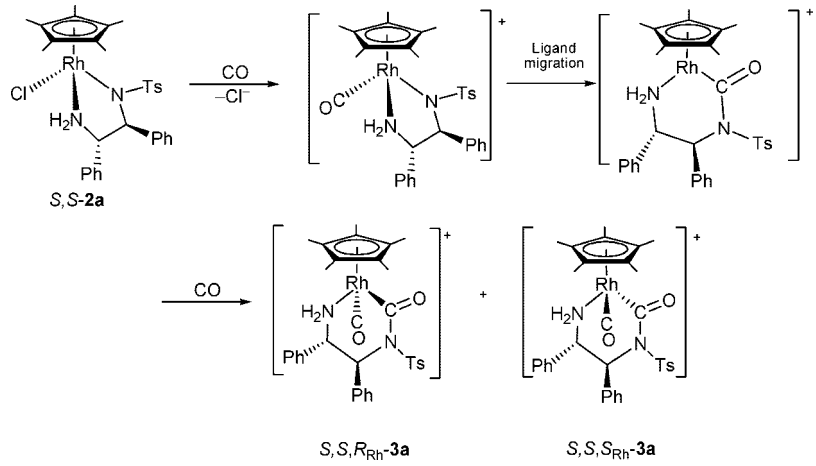

3). Both ESI and FAB mass spectrometry revealed peaks at $m/z = 603$ for $[M - 2CO]^+$; the parent molecular ion was not detected. Insertion of CO into mononuclear amido and amidinato complexes has been observed previously to form carbamoyl complexes.[45−48] Recently Rauchfuss et al. have reported a similar loss of chirality in related complexes, $[Cp^*Ir(L)(TsNCHPhCHPhNH_2]^+$ (L = PPh_3, $P(4\text{-}FC_6H_4)_3$, $P(4\text{-}MeOC_6H_4)_3$, or CO).[22]

On release of the pressure of CO from the NMR tube (before complete conversion to $Cp^*Rh(CO)_2$), **3a** converted back to **2a** sufficiently slowly to allow IR spectra to be recorded. The IR spectrum showed a peak at 2056 cm^{-1} consistent with a terminal CO ligand and a peak at 1600 cm^{-1} assigned to the acyl group of the bidentate ligand for **3a**. When ^{13}C-enriched CO was used, the peaks for the ^{13}C isotopomers were observed at 2003 cm^{-1} (2012 cm^{-1} calcd, based on the change in reduced mass) and 1562 cm^{-1} (1566 cm^{-1} calcd). The reaction between **2a** and CO may be accelerated by the presence of methanol. When complex **2a** was dissolved in CD_3OD with 3 atm of CO, the color changed immediately from orange to yellow. The NMR spectrum of the product solution was consistent with conversion to the two diastereoisomers of **3a**, as described for the reaction in CD_2Cl_2. The ^1H NMR spectrum (500 MHz, CD_3OD, 300 K) of **3a** showed two peaks for Cp* (δ 1.68 and 1.82), two for the tosyl methyl group (δ 2.25 and 2.31), a multiplet consistent with the CH protons of the ligand backbone at δ 4.48−4.52, and another at δ 5.03−5.08. Notably, the two isomers were formed initially with a 4:1 ratio (δ 1.68 dominant), but equalized in intensity after about an hour. This experiment therefore also suggests reversible CO coordination leading to thermodynamic equilibrium.

Recently, Ikariya et al. showed that the related cyclometalated iridium chloride complexes react with $AgBF_4$ and CO to form metal carbonyl cations with ν_{CO} very close to the values that we report for the terminal CO.[49] Rauchfuss and co-workers have reported the complexes $[Cp^*Ir(CO)(TsCH_2CH_2NH_2)][BF_4]$, $[Cp^*Ir(CO)(Ts\text{-}1,2\text{-}C_6H_{10}NH_2)][BF_4]$, and $[Cp^*Ir(CO)(TsCHPhCHPhNH_2)][BF_4]$ with ν_{CO} of 2059, 2059, and 2064 cm^{-1}.[21,22]

Reaction of **2a** with *t*BuNC in CH_3OH gives an immediate color change to yellow; extraction into toluene followed by addition of KPF_6 yields $[Cp^*Rh(CNtBu)(TsNCHPhCHPhNH_2)][PF_6]$ (**4a**) as a yellow powder (Scheme 4). The complex was crystallized from THF/hexane to give **4a** as yellow needles. The IR spectrum shows ν_{CN} at 2112 cm^{-1} (KBr disk). The ^{13}C NMR spectrum shows a resonance for *t*BuN*C* at δ 134.8 as a doublet of multiplets with $J_{RhC} = 69$ Hz. These data are consistent with those for $Cp^*RhCl_2(CNMe)$, which exhibits a doublet of triplets at δ 136.3 with $J_{RhC} = 69$ Hz and $J_{NC} = 20$ Hz.[50]

Scheme 4. Reactions of 2a with *t*BuNC, HCO_2H, LiBr, and KI

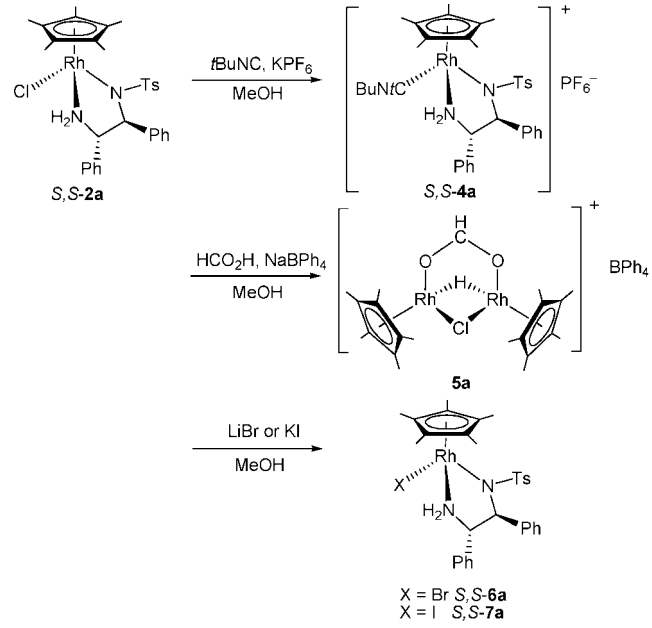

The reaction of **2a** with HCO_2H (10 equiv) in methanol was performed to establish how **2a** reacts with a single component of the system for catalytic transfer hydrogenation. Upon addition of formic acid, the color of the solution turned immediately from orange to red, and a red powder was isolated by adding 2 equiv of $NaBPh_4$ to a solution of the metal complex in methanol. ESI mass spectrometry ($M^+ = 557$) was consistent with formation of the triply bridged dimer $[\{Cp^*Rh\}_2(\mu\text{-}H)(\mu\text{-}Cl)(\mu\text{-}HCO_2)][BPh_4]$ (**[5a][BPh4]**), and this assignment was con-

(45) Piraino, P.; Bruno, G.; Tresoldi, G.; Farone, G.; Bombieri, G. *J. Chem. Soc., Dalton. Trans.* **1983**, 2391.
(46) Bryndza, H. E.; Fultz, W. C.; Tam, W. *Organometallics* **1985**, *4*, 939.
(47) Joslin, F. L.; Johnson, M. P.; Mague, J. T.; Roundhill, D. M. *Organometallics* **1991**, *10*, 2781.
(48) Rahim, M.; Ahmed, K. J. *Organometallics* **1994**, *13*, 1751.
(49) Arita, S.; Koike, T.; Kayaki, Y.; Ikariya, T. *Organometallics* **2008**, *27*, 2795.
(50) Jones, W. D.; Duttweiler, R. P.; Feher, F. J. *Inorg. Chem.* **1990**, *29*, 1505.

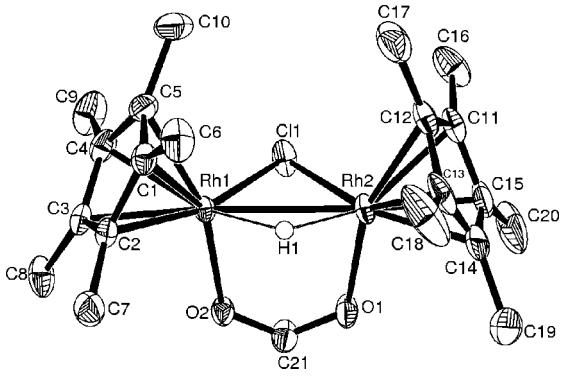

Figure 6. Molecular structure of the cation in **[5a][BPh$_4$]·OEt$_2$** (thermal ellipsoids shown at 50% probability). Hydrogen atoms are omitted except for hydride. Selected bond lengths [Å] and angles [deg]: Rh(1)···Rh(2) 2.8251(3), Rh(1)−O(2) 2.1044(18), Rh(2)−O(1) 2.117(2), Rh(1)−H(1) 1.73(3), Rh(2)−H(1) 1.77(3), Rh(1)−Cl(1) 2.4290(7), Rh(2)−Cl(1) 2.4201(7); Rh(1)−Cl(1)−Rh(2) 71.27(2), Rh(1)−O(2)−C(21) 123.79(18), Rh(2)−O(1)−C(21) 123.25(18), O(1)−C(21)−O(2) 128.3(3).

firmed by X-ray analysis using a crystal grown from acetone/Et_2O at −20 °C (Scheme 4). Related triply bridged cationic dimers of general formula [{Cp*Rh}$_2$(μ-H)(μ-OCOR)$_2$][PF$_6$] have been reported by Maitlis et al.[51]

The crystal structure of **[5a][BPh$_4$]·OEt$_2$** (Figure 6) reveals Rh(1)−O(2) and Rh(2)−O(1) distances of 2.1044(18) and 2.117(2) Å, respectively, longer than those in [{Cp*Rh}$_2$(μ-H)$_2$(μ-CO$_2$CH$_3$)]$^+$ (2.071 and 2.070 Å).[52] The hydride in the cation **5a** was readily located on a difference map. Rh(1)−H(1) and Rh(2)−H(1) distances of 1.73(3) and 1.77(3) Å, respectively, are comparable to those in [{Cp*Rh}$_2$(μ-H)$_2$(μ-CO$_2$CH$_3$)]$^+$ (1.73 Å). The geometry of the bridge is different from that of its analogues. The Rh···Rh distance for the cation **5a** of 2.8251(3) Å may be compared with 2.680 Å in [{Cp*Rh}$_2$(μ-H)$_2$(μ-CO$_2$CH$_3$)]$^+$.[52] The average Rh(1)−Cl distance of 2.425(1) Å is shorter than that in [{Cp*Rh}$_2$(μ-Cl)$_3$]$^+$ (2.457 Å),[53] while the Rh(1)−Cl(1)−Rh(2) angle of 71.27(2)° for **5a** is much more acute than that for [{Cp*Rh}$_2$(μ-Cl)$_3$]$^+$ (81.23° average). The O(1)−C(21)−O(2) angle of 128.3(3)° is wider than that of [{Cp*Rh}$_2$(μ-H)$_2$(μ-CO$_2$CH$_3$)]$^+$ (124.80°).

The ^{1}H NMR spectrum (500 MHz, $(CD_3)_2CO$, 300 K) of **[5a][BPh$_4$]** showed a triplet at δ −8.67 (J_{RhH} = 27 Hz) for the bridging hydride, a singlet at δ 1.83 for the Cp* protons, and a triplet at δ 7.41 (J_{RhH} = 4 Hz) for the bridging formate proton.

The isolation of **[5a][BPh$_4$]** raises the question of whether cation **5a** could be formed under catalytic conditions when the formic acid is buffered by triethylamine. As an experimental test, we investigated the reduction of d_6-acetone by d_{15}-triethylamine/formic acid catalyzed by **2a** in CD_3CN solution. The molar ratio of acetone substrate to catalyst was 20:1. The reaction was carried out both at 250 K and at 300 K with the same result. Examination of the hydride region of the ^{1}H NMR spectrum showed one hydride species only with a triplet at δ −8.76 (J = 27 Hz), consistent with significant formation of the hydride-bridged cation **5a**. The same species was observed with CD_3OD and CD_2Cl_2 as solvents.

The surprising observation of **5a** under catalytic conditions raises the question of whether reaction of the catalyst with formic acid is a significant deactivation pathway. We compared the catalytic activities of **2a** and **[5a][BPh$_4$]** for the transfer hydrogenation of the imine 6,7-dimethoxy-1-methyl-3,4-dihydroisoquinoline. Under conditions when **2a** gave excellent activity and ee's of 90%,[20,54] complex **[5a][BPh$_4$]** showed very poor activity. However, the catalytic system of {**5a** + **1a**} gave activity and selectivity comparable to that of **2a**. Thus we conclude that reaction of **2a** with formic acid to form **5a** may occur to some extent under catalytic conditions despite the presence of NEt_3. Nevertheless, catalytic activity is not necessarily blocked because the presence of free chiral ligand may allow recovery of activity.

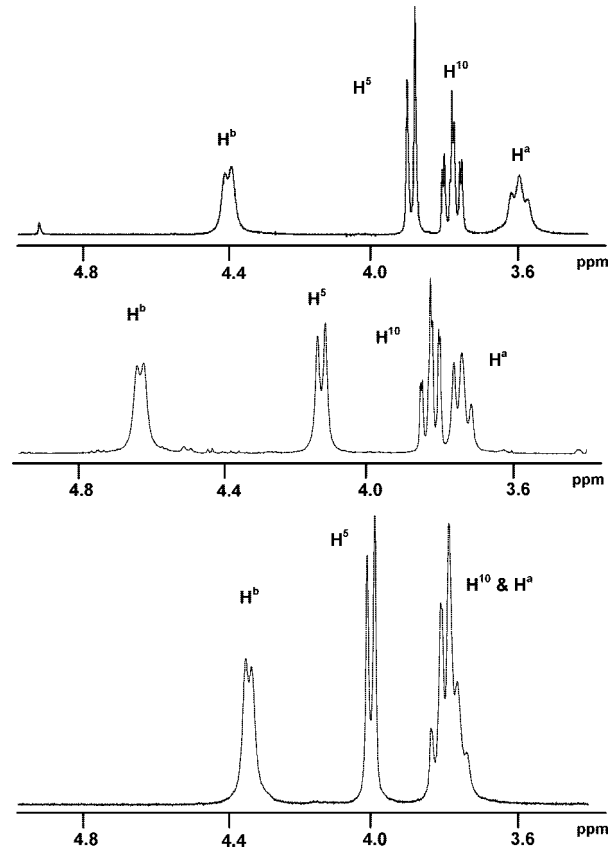

Figure 7. ^{1}H NMR (C*H*Ph and NH_2 region) spectra of **2a** (top), **6a** (middle), and **7a** (bottom) 500 MHz, CD_3CN, 300 K.

2. Reactions with Halide Salts. The addition of LiBr or KI to a solution of *S*,*S*-**2a** in methanol resulted in quantitative conversion to the corresponding bromide Cp*RhBr(S,S-TsNCHPhCHPhNH$_2$) (*S*,*S*-**6a**) or iodide Cp*RhI(S,S-TsNCHPhCHPhNH$_2$) (*S*,*S*-**7a**), respectively (Scheme 4). The addition of iodide salts is accompanied by a color change from pale orange to dark red. Both complexes were characterized by ^{1}H and ^{13}C NMR spectroscopy, FAB mass spectrometry, and X-ray crystallography. The ^{1}H NMR spectra show most variation between **2a**, **6a**, and **7a** in the proton chemical shifts of the ligand backbone and NH_2 groups, as illustrated in Figure 7.

Complex *S*,*S*-**6a** was recrystallized by slow diffusion of hexane into a concentrated solution in THF. Crystals of *S*,*S*-**7a**·CH_3OH were obtained by slow evaporation of a solution in CH_3OH. Selected bond lengths, angles, and interatomic distances are compared to those for **2c** and literature values for **2a** and for **Ru** ((*p*-cymene)RuCl(TsNCHPhCHPhNH$_2$)) in Table 1. The

(51) Cook, J.; Hamlin, J. E.; Nutton, A.; Maitlis, P. M. *J. Chem. Soc., Dalton. Trans.* **1981**, 2342.

(52) Nutton, A.; Bailey, P. M.; Maitlis, P. M. *J. Organomet. Chem.* **1981**, *213*, 313.

(53) Gauthier, S.; Quebatte, L.; Scopelliti, R.; Severin, K. *Inorg. Chem. Commun.* **2004**, *7*, 708.

(54) Grace, J. The Rh catalysed asymmetric transfer hydrogenation of Imines; a mechanistic study. Ph.D. Thesis, University of York, 2007.

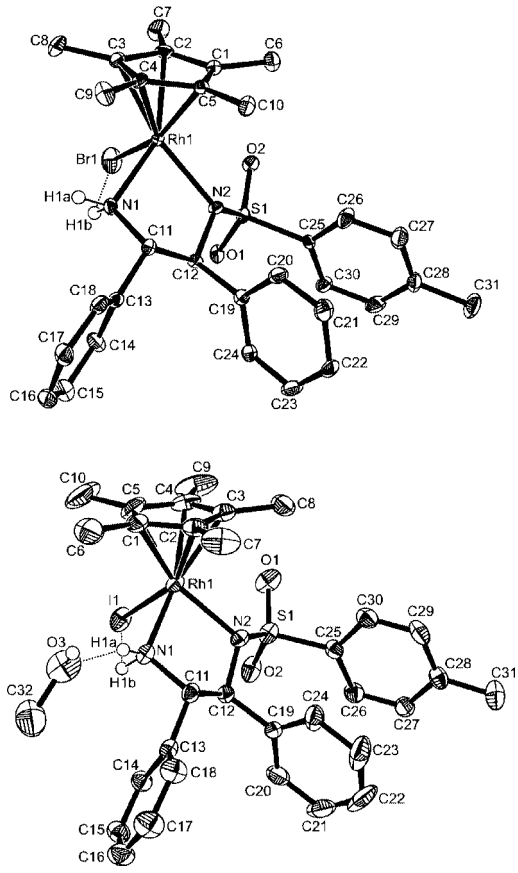

Figure 8. Molecular structures of *S,S*-**6a** (above) and *S,S*-**7a·CH$_3$OH** (below) (thermal ellipsoids shown at 50% probability). Hydrogen atoms are omitted except for the amino group and methanol OH. The hydrogen bonds are shown as dotted lines.

amine hydrogen atoms were located by difference maps; their positions were refined successfully for **7a** but their positions were constrained in the refinement of **6a**. The structures of **2a**, **2c**, **6a**, and **7a** are very similar and also close to that of **Ru**.[3] The most important features are (a) that the Rh−N(1) (NH_2) bond is significantly shorter than the Rh−N(2) (NS) bond and (b) that each complex possesses an intramolecular NH···X hydrogen bond. The phenyl groups lie in equatorial positions on the five-membered Rh−N−C−C−N ring, as in related structures and in agreement with the evidence provided by the ^{1}H NMR data (see above).[22] The Rh−NH_2 bond length is invariably shorter than the Rh−NS bond length, but the differences Δr(M−N) are larger for **2a** and **6a** (0.081(8) and 0.085(6) Å) than for **2c** and **7a** (0.058(2) and 0.046(4) Å). The changes arise from an increased Rh−N(1) and decreased Rh−N(2) distance in **7a** and a decreased Rh−N(2) distance in **2c**. The esd on Δr(M−N) for the ruthenium complex is too large to compare to the values for the other complexes with confidence. The N···X and NH···X distances are consistent with an NH···X hydrogen bond in each complex (X = Cl, Br, I). The NH···X distances are shorter than the sum of the van der Waals radii by 0.40, 0.44, and 0.40 Å in **2c**, **6a**, and **7a**, respectively (van der Waals radii of Cl 1.75, Br 1.85, I 1.98, and H 1.20 Å).[55,56] Complex **7a** crystallizes as the methanol solvate and exhibits a further hydrogen bond between the methanol oxygen and the NH hydrogen that does not interact with iodine (Figure 8). In **2c**, there are also short S=O(1)···HC(30) and S=O(1)···HC(12) contacts with O···C of 2.881(3) and 2.899(2) Å, respectively. The intramolecular hydrogen bonds have been noted in previous structures, but the striking difference in the Rh−N distances has not been emphasized, perhaps because the esd's on the older structures were larger than on those reported here.[3,5,15]

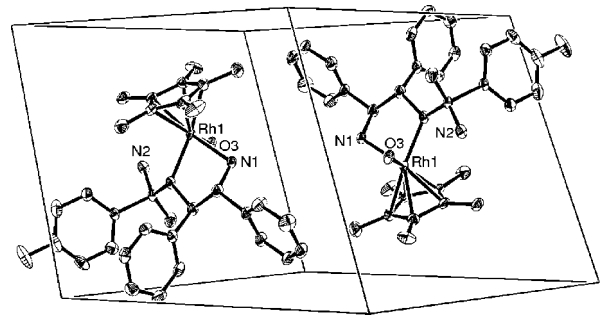

Figure 9. Molecular structure and unit cell for **[8c-H$_2$O][OTf]** (thermal ellipsoids shown at 50% probability). Hydrogen atoms and anions are omitted for clarity. Selected bond lengths [Å] and angles [deg]: Rh(1)−N(1) 2.1328(19), Rh(1)−O(3) 2.1631(18), Rh(1)−N(2) 2.141(2); N(1)−Rh(1)−N(2) 77.61(8), N(1)−Rh(1)−O(3) 85.24(7), N(2)−Rh(1)−O(3) 90.08(7).

3. Halide Abstraction. In an attempt to provide a route to a crystalline analogue of the CO complex **3a**, the reaction of *S,S*-**2c** with AgOTf (OTf = CF_3SO_3) in CH_3OH was carried out. The chloride abstraction succeeded although the CO reaction proved unsuccessful; the addition of AgOTf to a solution of **2c** in methanol led to an immediate color change from orange to magenta and precipitation of AgCl. After filtering off the insoluble salt and removing the solvent under reduced pressure, a purple solid was obtained. This solid was identified as [Cp*Rh(4-$FC_6H_4SO_2$NCHPhCHPhNH_2)][OTf] (**[8c][OTf]**). A sample was dissolved in CD_3CN for NMR analysis, resulting in a yellow solution, suggesting CD_3CN coordination to Rh. Attempts to locate the coordinated CH_3CN by running a ^{1}H NMR spectrum in CH_3CN using solvent suppression were unsuccessful, although exchange could be occurring on the NMR time scale. The coordination of solvent was supported by an IR band at 2239 cm^{-1} consistent with the CN stretch of coordinated CH_3CN.[57]

Complex **[8c][OTf]** was characterized by ^{1}H, ^{13}C, and ^{19}F NMR spectroscopy in CD_3CN. The ^{1}H NMR spectrum displayed peaks at δ 4.50 and 3.95 for the NH_2 protons, a resonance at δ 1.83 for Cp*, and signals at δ 4.15 and δ 3.76 for the C*H*Ph protons. The ^{13}C NMR resonances of the sulfonyl aromatic ring carbons all show couplings to ^{19}F, as for **2c**. A diffuse reflectance UV−vis spectrum of **[8c][OTf]** showed λ_{max} = 520 nm. The ESI mass spectrum in CH_3OH showed the expected peak at m/z = 607 for $[M]^+$, without coordinated solvent.

A crystal suitable for X-ray analysis was grown by vapor diffusion of hexane into a solution of **[8c][OTf]** in CH_3OH/toluene (1:1). The structure obtained was a derivative of **[8c][OTf]** with a water molecule coordinated to the rhodium center, **[8c-H$_2$O][OTf]** (Figure 9). The most significant difference in the structure of **[8c-H$_2$O][OTf]** from those of **2a** and **2c** is a change from a chiral to an achiral space group. Complex **[8c-H$_2$O][OTf]** crystallized in the achiral space group $P\bar{1}$, whereas those used to solve structures of **2a**−**2c** were the chiral space groups $P2_1$ or $P2_12_12_1$. The hydrogen atoms of the coordinated water and amine were located in a difference map

(55) Rowland, R. S.; Taylor, R. *J. Phys. Chem.* **1996**, *100*, 7384.
(56) Bondi, A. *J. Phys. Chem.* **1964**, *68*, 441.
(57) Rigby, W.; Bailey, P. M.; McCleverty, J. A.; Maitlis, P. M. *J. Chem. Soc., Dalton. Trans.* **1979**, 371.

and refined isotropically. Figure 9 shows that the two molecules in the cell have opposite chirality at both Rh and ligand, and it appears that the ligand has racemized. At the molecular level, there are also important changes: the Rh−NH_2 distance in **[8c-H_2O][OTf]** is 0.026(3) Å longer than in **2c**, while the Rh−NTs distance is 0.024(3) Å shorter, with the result that Δr(Rh−N) is insignificant. The Rh−O bond in **[8c-H_2O][OTf]** of 2.1631(18) Å is comparable to the mean value in [Cp*Rh$(OH_2)_3$][OTf]$_2$ (2.156 Å)[58] and that in [Cp*Rh$(PMe_3)(OH_2)(C_6F_5CF_2)$][$BF_4$] (2.164(7) Å).[59] The amine hydrogen atoms engage in hydrogen bonding to the oxygen atoms of the triflate counterion, while the water hydrogen atoms form hydrogen bonds with the fluorine and oxygen atoms of the counterion and with the sulfonyl oxygens.

The crystal structure leaves the question open whether the majority of the complex has racemized or whether the result depends on the selection of crystals. Further evidence for racemization of the TsDPEN ligand was obtained by measuring the optical rotation of a solution of *S,S*-**2c** in $CHCl_3$, reacting this with AgOTf to form **[8c][OTf]**, and measuring the optical rotation of the resulting solution at constant concentration. The solution of complex *S,S*-**2c** had an optical rotation of −1.5°, whereas the solution of the product **[8c-H_2O][OTf]** had an optical rotation of −0.1°. Furthermore, subsequent conversion of **[8c-H_2O][OTf]** back to **2c** (via addition of Bu_4NCl) resulted in an optical rotation of −0.6°, well short of the initial optical rotation. This significant reduction of optical activity for the product solution is evidence that a substantial proportion of the ligand in the complex has racemized and the effect is not confined to a few crystals.

A second crop of crystals of **[8c][OTf]** was grown as described above, but under anhydrous conditions, and proved to have a different structure. In the absence of water or a suitable coordinating solvent, the cationic 16-electron complex dimerized. Although the structure is of poor quality, the principal features are important. An oxygen of the sulfonyl group of one molecule has filled the vacant site at that of the other and *vice versa* to give the dimer [Cp*Rh(4-$FC_6H_4SO_2$NCHPhCHPhNH$_2$)]$_2$[OTf]$_2$ (**[8c]$_2$[OTf]$_2$**, structure below). As with **[8c-H_2O][OTf]**, the structure of **[8c]$_2$[OTf]$_2$** was solved with the achiral $P\bar{1}$ space group and opposite enantiomers are paired in the unit cell. For comparison, [Cp*Rh(R^{1}COCHCOR^2)][PF_6] has been shown to exist as a dimer by coordination of the central acetylacetonate carbon of one complex to Rh in another and *vice versa*.[60] An ESI mass spectrum of [**8c][OTf]** showed a significant peak at m/z = 1363 for [$M_2(SO_3CF_3)$]$^+$, providing some evidence for the existence of the dimer in solution as well as in the solid state.

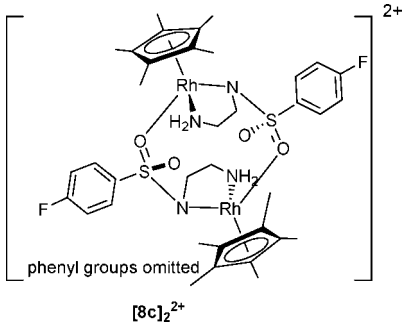

[8c]$_2^{2+}$

The racemization of the ligand in **[8c-H_2O][OTf]** is of importance in asymmetric transfer hydrogenation. A possible mechanism for this racemization of the ligand is outlined (Scheme 5): step 1 is the reversible dissociation of coordinated

Scheme 5. Possible Mechanism for the Racemization of the FsNCHPhCHPhNH$_2$ Ligand in [8c-S]$^+$ (S, = solvent, Fs = 4-$FC_6H_4SO_2$)

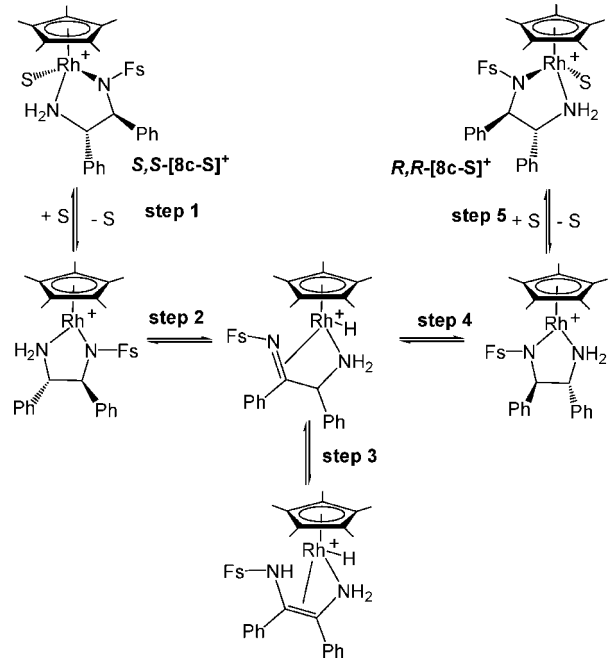

solvent; step 2 is a β-elimination; step 3 is an imine−enamine tautomerism, which scrambles the chirality; steps 4 and 5 are the reverse of steps 1 and 2, so both enantiomers are as likely to be formed and a racemic mixture ensues. The *meso* isomer is likely to be much higher in energy and disfavored. This mechanism remains unproven, but it provides a plausible explanation of the observations.

The reactivity of **[8c][OTf]** toward two-electron donors was studied as a route to new cationic Rh complexes; although the reaction with CO was unsuccessful, an adduct was formed by reaction with *t*BuNC. Upon addition of 1 equiv of *t*BuNC to a solution of **8c** in CH_3OH, an immediate color change from magenta to yellow was observed. Workup by removing the solvent under reduced pressure, extraction into CH_3CN, and removal of CH_3CN under vacuum gave a yellow solid, which has been characterized by ^{1}H, ^{13}C, and ^{19}F NMR spectroscopy and ESI mass spectrometry and was found to be [Cp*Rh(CN*t*Bu)(4-$FC_6H_4SO_2$NCHPhCHPhNH$_2$)][OTf] (**4c**).

Conclusions

A group of 18-electron half-sandwich rhodium complexes, of the type [Cp*Rh(X)(4-$RC_6H_4SO_2$NCHPhCHPhNH$_2$)] (X = Cl, Br, I; R = Me, *t*Bu, F), of significance in asymmetric transfer hydrogenation catalysis[5−7,10,15,17,20] has been isolated. The complexes have been characterized by multinuclear NMR spectroscopy and by X-ray crystallography. The NMR spectra show significant solvent dependence of the ^{1}H chemical shift of the NH_2 protons characteristic of NH···X hydrogen bonding. The ^{1}H–^{15}N HMQC NMR spectra show that the chemical shifts of the inequivalent nitrogen atoms are separated by ca. 50 ppm; moreover, the resonances exhibit significant coupling to the C_5Me_5 protons and to the rhodium nucleus. These methods offer scope for wider application for characterization of the nitrogen environment in solution. Notable features of the X-ray structure are the significantly longer Rh−N bonds to the amido nitrogen than the amino nitrogen and the presence of an intramolecular

Table 2. Crystallographic Data for 2c, [5a][BPh_4]·OEt_2, 6a, 7a, and [8c·H_2O][OTf]

	2c	[5a][BPh_4]·OEt_2	6a	7a	[8c-H_2O][OTf]
formula	$C_{30}H_{33}ClFN_2O_2RhS$	$C_{49}H_{62}BClO_3Rh_2$	$C_{31}H_{36}BrN_2O_2RhS$	$C_{32}H_{40}IN_2O_3RhS$	$C_{34.5}H_{38.5}F_4N_2O_6RhS_2$
M	643.00	951.07	683.50	762.53	820.20
a/Å	7.8845(4)	11.7528(10)	8.3927(4)	8.4842(5)	12.286(5)
b/Å	11.3176(5)	13.6373(12)	16.1471(8)	9.1856(6)	12.454(5)
c/Å	31.7839(14)	14.2877(12)	21.6575(11)	20.6402(13)	13.377(5)
α/deg		106.264(2)			107.266(7)
β/deg		92.571(2)		97.4630(10)	113.603(7)
γ/deg		92.506(2)			97.270(7)
V/Å^3	2836.2(2)	2192.3(3)	2935.0(3)	1594.92(17)	1719.2(12)
T/K	100(2)	110(2)	110(2)	110(2)	110(2)
space group	$P2_12_12_1$	$P\bar{1}$	$P2_12_12_1$	$P2_1$	$P\bar{1}$
Z	4	2	4	2	2
μ(Mo Kα)/mm^{-1}	0.807	0.854	2.045	1.603	0.688
reflns measd	42 801	22 323	32 890	21 931	23 383
reflns indep	8180	10 753	8364	7863	8538
R_{int}	0.0289	0.0221	0.0803	0.0244	0.0267
final $R[I > 2\sigma(I)]$	$R_1 = 0.0254$	$R_1 = 0.0351$	$R_1 = 0.0429$	$R_1 = 0.0248$	$R_1 = 0.0336$
	$wR_2 = 0.0625$	$wR_2 = 0.0847$	$wR_2 = 0.1177$	$wR_2 = 0.0585$	$wR_2 = 0.0848$
final R (all data)	$R_1 = 0.0268$	$R_1 = 0.0440$	$R_1 = 0.0548$	$R_1 = 0.0272$	$R_1 = 0.0380$
-	$wR_2 = 0.0672$	$wR_2 = 0.0889$	$wR_2 = 0.1212$	$wR_2 = 0.0663$	$wR_2 = 0.0869$
CCDC number	703218	703216	703215	703214	703217

NH···X hydrogen bond that may prepare the complex for proton abstraction.[3,5,15]

Direct reaction of Cp*Rh(Cl)(*S,S*-TsNCHPhCHPhNH$_2$) with CO results in the reversible formation of [Cp*Rh(CO)-{C(O)N(Ts)CHPhCHPhNH$_2$}][Cl] as two diastereomers, *S,S,*R_{Rh} and *S,S,*S_{Rh}, with different configurations at rhodium. This species has been identified by 2D-^{13}C−^{13}C NMR spectroscopy with ^{13}CO labeling and by IR spectroscopy. The growth of the second isomer may be monitored during reaction in d_4-methanol as solvent. Further reaction with CO leads to the complete displacement of the nitrogen ligands. The nitrogen ligands are also completely displaced by reaction of **2a** with formic acid, yielding dinuclear [{Cp*Rh}$_2$(μ-H)(μ-Cl)(μ-HCO$_2$)][BPh_4], **[5a][BPh_4]**, closely related to carboxylate complexes observed previously.[51] Cation **5a** is also detected under catalytic conditions for reduction of d_6-acetone with d_{15}-NEt_3 and formic acid; that is, the buffering effect of triethylamine is not sufficient to prevent some reaction. Although formation of complex **[5a][BPh_4]** represents a deactivation path for the catalyst, catalytic activity can be recovered by reaction of **[5a][BPh_4]** with the ligand **1a**.

Reaction of Cp*RhCl(*S,S*-4-FC$_6$H$_4$SO$_2$NCHPhCHPhNH$_2$) with AgOTf generates a purple 16-electron complex that exists as the dimer [Cp*Rh(4-FC$_6$H$_4$SO$_2$NCHPhCHPhNH$_2$)]$_2$[OTf]$_2$ in the crystalline state. In the presence of adventitious water, it is isolated as a salt of the aqua cation [Cp*Rh(4-FC$_6$H$_4$SO$_2$-NCHPhCHPhNH$_2$)(OH$_2$)][OTf]. The notable feature of this reaction is that it results in racemization of both CHPh centers (i.e., formation of a mixture of *R,R* and *S,S* from initial *S,S* material). Thus halide abstraction in this manner would result in loss of enantioselectivity of the catalyst.

Experimental Section

General Procedure. Unless otherwise stated, synthetic work was carried out in air with untreated solvents. Commercially available reagents were obtained from the following sources: [Cp*RhCl$_2$]$_2$, *R,R* and *S,S*-DPEN, *R,R* and *S,S*-TsDPEN, 6,7-dimethoxy-3,4-dihydroisoquinoline (donated by Piramal Healthcare); RhCl$_3$·xH$_2$O (Precious Metals Online); hexamethyl(dewar)benzene, benzil, 4-fluorobenzenesulfonyl chloride, 4-*tert*-butylbenzenesulfonyl chloride, triethylamine, lithium, ammonium-^{15}N acetate (98 atom % ^{15}N), formic acid (Aldrich); tosyl chloride (Alfa Aesar); d_{15}-triethylamine from Cambridge Isotope Laboratories. Ar, N_2, CO, and H_2 gases (BOC) and were used as received without further purification. [Cp*RhCl$_2$]$_2$ was also made as previously reported.[61] When necessary, dry solvents (Fisher Scientific AR or HPLC grade) were prepared by refluxing over Mg/I_2 (CH_3OH), CaH_2 (CH_3CN, CH_2Cl_2), or sodium/benzophenone (THF) and were degassed and, along with air- and moisture-sensitive materials, stored under a dry Ar atmosphere. Manipulations of these compounds were performed using standard Schlenk, high-vacuum, and glovebox techniques. Deuterated solvents (Aldrich) were dried using CaH_2 (CD_3OH, CD_3CN, and CD_2Cl_2) and degassed by three freeze−pump−thaw cycles.

Unless otherwise stated, DPEN, TsDPEN, 4-FC$_6$H$_4$SO$_2$DPEN, 4-*t*BuC$_6$H$_4$SO$_2$DPEN, and all metal complexes have been synthesized and used as single diastereomers, with either the *R,R* or *S,S* configuration at the ligand, which, when coordinated to the metal, enforces the opposite chirality at Rh; the metal complex of the *S,S* ligand will have the *R* configuration at the metal center and *vice versa*. When referring to DPEN and related ligands, the specific chirality is not always mentioned, as both have been used interchangeably.

Most NMR spectra were recorded on Bruker AMX500, DRX400, or AMX300 spectrometers. The chemical shift values are reported relative to the residual protons of the deuterated solvent, according to the standard Bruker list. Numbering of hydrogen and carbon atoms refers to Figure 2. ^{1}H−^{103}Rh HMQC spectra were run on a Bruker Avance II 700 MHz spectrometer calibrated against [Cp*RhCl$_2$]$_2$ at δ 2303.[62] ^{1}H−^{15}N HMQC spectra were referenced to pyridine as δ 0. FAB mass spectra were recorded on a VG AutoSpec, and ESI mass spectra were recorded on a Thermo Electron LCQ Classic. Infrared spectra were recorded on a Unicam RS 10000E FTIR instrument. Polarimetry measurements were made in a Jasco DIP-370 digital polarimeter using a 2 mL cell and $CHCl_3$ solvent. Microanalysis was carried out by Elemental Microanalysis Ltd., Okehampton, Devon.

Synthesis of 4-RC$_6$H$_4$SO$_2$DPEN Ligands.[37] DPEN was dissolved in CH_2Cl_2 in a two-necked, 500 mL round-bottom flask. The solution was cooled to 0 °C, NEt_3 was added, and the mixture was stirred magnetically. The appropriate sulfonyl chloride was

(58) Eisen, M. S.; Haskel, A.; Chen, H.; Olmstead, M. M.; Smith, D. P.; Maestre, M. F.; Fish, R. H. *Organometallics* **1995**, *14*, 2806.
(59) Hughes, R. P.; Lindner, D. C.; Rheingold, A. L.; Liable-Sands, L. M. *J. Am. Chem. Soc.* **1997**, *119*, 11544.
(60) Rigby, W.; Lee, H. B.; Bailey, P. M.; McCleverty, J. A.; Maitlis, P. M. *J. Chem. Soc., Dalton. Trans.* **1979**, 387.
(61) Kang, J. W.; Moseley, K.; Maitlis, P. M. *J. Am. Chem. Soc.* **1969**, *91*, 5970.
(62) Tedesco, V.; von Philipsborn, W. *Magn. Reson. Chem.* **1996**, *34*, 373.

dissolved in CH_2Cl_2 and added to a dropping funnel, which was placed in the side neck of the round-bottom flask. The sulfonyl chloride solution was added to the stirred DPEN/NEt_3 solution dropwise over an hour, and the solution was warmed to room temperature and stirred overnight. It was washed successively with water (80 mL), $NaHCO_3$ solution (80 mL), water (80 mL), and brine (80 mL) and then dried over $MgSO_4$; the solvent was removed under reduced pressure to give a white solid, which was crystallized from EtOAc/hexane.

4-*t*BuC$_6$H$_4$SO$_2$DPEN (1b). 1b was synthesized as described above from DPEN (2.10 g, 9.9 mmol) and NEt_3 (2.10 mL, 14.9 mmol) in CH_2Cl_2 (150 mL) and 4-*tert*-butylbenzenesulfonyl chloride (2.00 g, 8.7 mmol) in CH_2Cl_2 (50 mL). Yield: 1.72 g (48%). ^{1}H NMR (500 MHz, CD_2Cl_2, 300 K, numbering as in Figure 2): δ 1.29 (9H, s, $(CH_3)_3C$), 4.14 (1H, d, J_{HH} = 5 Hz, H^5 or H^{10}), 4.35 (1H, d, J_{HH} = 5 Hz, H^5 or H^{10}), 7.12−7.15 (10H, m, Ph), 7.21 (2H, d, J_{HH} = 8 Hz, H^2), 7.33 (2H, d, J_{HH} = 8 Hz, H^3). ^{13}C NMR (125 MHz, CD_2Cl_2, 300 K): δ 31.36 (s, $(CH_3)_3C$), 35.36 (s, $(CH_3)_3C$), 61.0 (s, C^5 or C^{10}), 63.86 (s, C^5 or C^{10}), 126.10 (s, C^3 or C^4), 127.15 (s, C^3 or C^4), 127.17 (s, Ph), 127.60 (s, Ph), 127.81 (s, Ph), 128.70 (s, Ph), 128.83 (s, Ph), 129.99 (s, Ph), 137.60 (s, C^1), 140.15 (s, C^6 or C^{11}), 142.30 (s, C^6 or C^{11}), 156.08 (s, C^4). MS (FAB, *m*/*z*): 410 ([MH$^+$]). IR (KBr/cm^{-1}): 3356 (ν_{NH}), 3298 (ν_{NH}), 3291 (br, ν_{NH}). Anal. Calcd for $C_{24}H_{28}N_2O_2S$: C, 70.55; H, 6.91; N, 6.86. Found: C, 70.84; H, 7.08; N 6.87.

4-FC$_6$H$_4$SO$_2$DPEN (1c). 1c was synthesized as described above from DPEN (2.46 g, 11.6 mmol) and NEt_3 (2.40 mL, 17.4 mmol) in CH_2Cl_2 (150 mL) and 4-fluorobenzenesulfonyl chloride (2.00 g, 10.4 mmol) in CH_2Cl_2 (50 mL). Yield: 2.30 g (60%). ^{1}H NMR (500 MHz, CD_2Cl_2, 300 K, numbering as in Figure 2): δ 4.17 (1H, d, J_{HH} = 5 Hz, H^5 or H^{10}), 4.38 (1H, d, J_{HH} = 5 Hz, H^5 or H^{10}), 6.86 (2 H, apparent t, J_{HH} = 9 Hz, J_{HF} = 9 Hz, H^2), 7.17−7.20 (10H, m, Ph), 7.41 (2H, dd, J_{HH} = 9, J_{HF} = 5 Hz, H^3). ^{13}C NMR (125 MHz, CD_2Cl_2, 300 K): δ 60.86 (s, C^5 or C^{10}), 63.84 (s, C^5 or C^{10}), 116.18 (d, J_{FC} = 23 Hz, C^2), 127.06 (s, Ph), 127.55 (s, Ph), 128.00 (s, Ph), 128.04 (s, Ph), 128.84 (s, Ph), 128.94 (s, Ph), 129.96 (d, J_{FC} = 9 Hz, C^2), 136.91 (d, J_{FC} = 4 Hz, C^4), 140.09 (s, C^6 or C^{11}), 142.19 (s, C^6 or C^{11}), 165.09 (d, J_{FC} = 251 Hz, C^1). ^{19}F NMR (480 MHz, CD_2Cl_2, 300 K): δ −107.54 (s). MS (FAB, *m*/*z*): 371 ([MH]$^+$). IR (KBr/cm^{-1}): 3350 (ν_{NH}), 3338 (ν_{NH}), 3291 (ν_{NH}). Anal. Calcd for $C_{20}H_{19}FN_2O_2S$: C, 64.85; H, 5.17; N, 7.56. Found: C, 64.72; H, 5.16; N, 7.49.

^{15}N-Labeled DPEN.[42] A mixture of benzil (3.31 g, 15.8 mmol), cyclohexanone (1.63 mL,15.8 mmol), ammonium acetate (7.5 g ^{14}N and 5.24 g ^{15}N), and acetic acid (30 mL) was refluxed for 1 h. The cooled mixture was slowly poured into vigorously stirred water (50 mL) and stirred for an additional 2 h, then left overnight. The crystals formed were collected by filtration, washed with water (4 × 10 mL), and dried *in vacuo* to give 5-spirocyclohexyl-2,3-diphenyisoimidazole (**A**) (4.41 g, 97%), which was used in the next step without further purification. To a magnetically stirred solution of **A** (4.41 g, 15.3 mmol) in THF (20 mL) and NH_3 (25 mL) at −78 °C was added Li (601 mg, 85.9 mmol). Stirring was continued for 2 h and the reaction monitored by TLC, at which time all of the starting material had been consumed. Ammonium chloride (4.0 g) was added at −78 °C and the reaction mixture warmed very slowly to evaporate the NH_3. When the temperature of the reaction mixture reached 0 °C, water (20 mL) and Et_2O (20 mL) were added, the mixture was shaken, and the phases were separated. The aqueous phase was washed with Et_2O (3 × 20 mL), and the combined organic extracts were washed with brine (20 mL), dried over Na_2SO_4, filtered, and concentrated *in vacuo* to a volume of 15 mL. The resulting solution was cooled to 0 °C, 2 M HCl (15 mL) was added with vigorous stirring, and the solution was warmed to room temperature and stirred for 1 h. Water (30 mL) and CH_2Cl_2 (30 mL) were added, the mixture was shaken, and the phases were separated. The organic phase was washed with water (10 mL), and the combined aqueous phases were washed with CH_2Cl_2 (20 mL). The aqueous phase was treated with 2 M NaOH (20 mL) and extracted with CH_2Cl_2 (5 × 10 mL). The combined organic phases were dried over Na_2SO_4, filtered, and concentrated *in vacuo* to give ^{15}N-labeled DPEN (1.36 g, 44%). ^{1}H NMR (500 MHz, $CDCl_3$, 300 K): δ 1.98 (4H, s), 4.09 (2H, s), 7.17−7.33 (10H, m). MS (FAB, *m*/*z*): 213 ([MH]$^+$), 214 (singly labeled [MH]$^+$), 215 (doubly labeled [MH]$^+$).

^{15}N-Labeled TsDPEN (1a-^{15}N). 1a-^{15}N was synthesized as described above from ^{15}N-labeled DPEN (178 mg, 0.84 mmol), NEt_3 (150 μL, 1.1 mmol) in CH_2Cl_2 (30 mL), and tosyl chloride (122 mg, 0.64 mmol) in CH_2Cl_2 (15 mL). Yield: 109 mg (46%). ^{1}H NMR (500 MHz, $CDCl_3$, 300 K): δ 2.33 (3H, s, CH_3), 4.16 (1H, d, J_{HH} = 6 Hz, CHNH$_2$), 4.39 (1H, d, J_{HH} = 6 Hz, CHNTs), 6.98 (2H, d, J_{HH} = 8 Hz, H^4), 7.12−7.18 (10H, m, Ph) Ar, 7.32 (2H, d, J_{HH} = 8 Hz, H^2). MS (FAB, *m*/*z*, relative intensity): 367 (63, [MH]$^+$ ^{14}N/^{14}N/^{12}C/^{32}S isotopomer), 368 (100, [MH]$^{+14}$N/^{14}N/^{13}C/^{32}S, ^{14}N/^{15}N/^{12}C/^{32}S isotopomers), 369 (69, [MH]$^{+14}$N/^{14}N/^{12}C/^{34}S, ^{14}N/^{15}N/^{13}C/^{32}S, ^{15}N/^{15}N/^{12}C/^{32}S isotopomers), 370 (37, [MH]$^+$ ^{14}N/^{15}N/^{12}C/^{34}S, ^{15}N/^{15}N/^{13}C/^{32}S isotopomers), 371 (18, [MH]$^+$ ^{15}N/^{15}N/^{12}C/^{34}S isotopomer), 372 (6, [MH]$^+$ ^{15}N/^{15}N/^{13}C/^{34}S isotopomer).

General Synthesis for Cp*RhCl(4-RC$_6$H$_4$SO$_2$NCHPhCHPhNH$_2$).[17] [Cp*RhCl$_2$]$_2$ and 4-RC$_6$H$_4$SO$_2$DPEN were dissolved in CH_2Cl_2, NEt_3 was added dropwise with stirring, and the resulting solution was stirred for 1 h. The solution was washed with water, dried over $MgSO_4$, and crystallized from CH_2Cl_2/hexane as orange needles.

Cp*RhCl(TsNCHPhCHPhNH$_2$) (2a). [Cp*RhCl$_2$]$_2$ (2.0 g, 3.2 mmol), TsDPEN (2.4 g, 6.5 mmol), and NEt_3 (1.3 g, 12.9 mmol) were reacted in CH_2Cl_2 (120 mL), to give **2a** (4.2 g, 93%). ^{1}H NMR (500 MHz, $CDCl_3$, 300 K, numbering as in Figure 2): δ 1.80 (15H, s, C_5Me_5), 2.21 (3H, s, Me), 3.46 (1H, br d, J_{HH} ≈ 11 Hz, NH^b), 3.70 (1H, ddd, J_{HH} = 3, 12, 14 Hz, H^{10}), 3.84 (1H, br apparent t, J_{HH} ≈ 12, 12 Hz, NH^a), 3.95 (1H, d, J_{HH} = 11 Hz, H^5), 6.64 (2H, d, J_{HH} = 7 Hz, H^7 or H^8), 6.76 (2H, t, J_{HH} = 7 Hz, H^7 or H^8), 6.80−6.85 (5H, m, H^3, H^9, and H^{12}), 7.09−7.14 (3H, m, H^{13} and H^{14}), 7.29 (2H, d, H^2). ^{13}C NMR (125 MHz, CD_2Cl_2, 300 K): δ 9.97 (s, C_5Me_5) 21.40 (s, Me), 69.91 (s, C^5), 72.05 (s, C^{10}), 94.92 (d, J_{RhC} = 8 Hz, C_5Me_5), 126.83 (s, C^3, C^9, or C^{13}), 127.54 (s, C^7 or C^8), 127.59 (s, C^3, C^9, or C^{13}), 128.27 (s, C^3, C^9, or C^{13}), 128.49 (s, C^2), 128.78 (s, C^{13} or C^{14}), 128.97 (s, C^{13} or C^{14}), 129.34 (s, C^7 or C^8), 139.79 (s, C^1), 140.06 (s, C^6 or C^{11}), 140.29 (s, C^6 or C^{11}), 142.27 (s, C^4). ^{15}N NMR (50.7 MHz, CD_2Cl_2, 300 K): δ −263.6 (d, J_{RhN} = 14 Hz, NH$_2$), −210.6 (d, J_{RhN} = 18 Hz, NTs). ^{103}Rh−^{1}H HMQC (22.18 MHz, $CDCl_3$, 300 K): δ 2550.5. MS (FAB, *m*/*z*): 639 ([MH]$^+$). IR (KBr/ cm^{-1}): 3281 (ν_{NH}), 3209 (ν_{NH}).

^{1}H NMR (500 MHz, CD_3CN, 300 K): δ 1.80 (15H, s, C_5Me_5), 2.24 (3H, s, Me), 3.60 (1H, br apparent t, J_{HH} ≈ 12, 12 Hz, NH^a), 3.78 (1H, ddd, J_{HH} = 3, 11, 14 Hz, H^{10}), 3.91 (1H, d, J_{HH} = 11 Hz, H^5), 4.41 (1H, br d, J_{HH} ≈ 9 Hz, NH^b), 6.68 (2H, d, J_{HH} = 8 Hz, H^7 or H^8), 6.77 (2H, t, J_{HH} = 7 Hz, H^7 or H^8), 6.83−6.88 (5H, m, H^3, H^9, and H^{12}), 7.11−7.14 (3H, m, H^{13} and H^{14}), 7.32 (2H, d J_{HH} = 8 Hz, H^2).

Cp*RhCl(4-*t*BuC$_6$H$_4$SO$_2$NCHPhCHPhNH$_2$) (2b). [Cp*RhCl$_2$]$_2$ (0.76 g, 1.23 mmol), 4-*t*BuC$_6$H$_4$SO$_2$DPEN (1.0 g, 2.45 mmol), and NEt_3 (0.68 mL, 4.9 mmol) were reacted in CH_2Cl_2 (50 mL) to give **2b** (1.0 g, 60%). Crystals suitable for X-ray analysis were grown by slow diffusion of hexane into a concentrated solution of **2b** in CH_2Cl_2. ^{1}H NMR (500 MHz, CD_2Cl_2, 300 K, numbering as in Figure 2): δ 1.21 (9H, s, CMe_3), 1.80 (15H, s, C_5Me_5), 3.47 (1H, br d, J_{HH} ≈ 10 Hz, NH^b), 3.69 (1H, ddd, J_{HH} = 3, 12, 14 Hz, H^{10}), 3.90 (1H, br apparent t, J_{HH} ≈ 11, 11 Hz, NH^a), 4.07 (1H, d, J_{HH} = 11 Hz, H^5), 6.59 (2H, d, J_{HH} = 7 Hz, H^7), 6.66 (2H, t, J_{HH} = 8 Hz, H^8), 6.71−6.74 (1H, m, H^9), 6.85−6.87 (1H, m, H^{12}), 6.96 (2H, d, J_{HH} = 10 Hz, H^2), 7.08−7.14 (3H, m, H^{13} and H^{14}), 7.23 (2H, d, J_{HH} = 9 Hz, H^3). ^{13}C (125 MHz, CD_2Cl_2, 300 K): δ 9.96

(s, C_5Me_5), 31.40 (s, CMe_3), 69.75 (s, C^5), 71.90 (s, C^{10}), 99.48 (d, J_{RhC} = 9 Hz, C_5Me_5), 124.60 (s, C^2), 126.96 (s, C^9), 127.53 (s, C^8), 127.84 (s, C^{12}), 127.86 (s, C^3), 128.76 (s, C^{13} or C^{14}), 128.96 (s, C^{13} or C^{14}), 129.35 (s, C^7), 139.72 (s, C^6 or C^{11}), 140.12 (s, C^6 or C^{11}), 143.02 (s, C^4), 152.53 (s, C^1). ^{15}N NMR (50.7 MHz, CD_2Cl_2, 300 K): δ −263.7 (d, J_{RhN} = 17 Hz, NH_2), −208.6 (d, J_{RhN} = 20 Hz, NTs). MS (FAB, *m*/*z*): 681 ([MH^+]). IR (KBr/cm^{-1}): 3287 (ν_{NH}), 3233 (ν_{NH}). Anal. Calcd for $C_{34}H_{42}ClN_2O_2RhS$: C, 59.95; H, 6.22; N, 4.11. Found: C, 59.70; H, 6.25; N, 4.16.

^{1}H NMR (500 MHz, CD_3CN, 300 K): δ 1.24 (9H, s, CMe_3), 1.80 (15H, s, C_5Me_5), 3.64 (1H, br apparent t, J_{HH} = 11, 11 Hz, NH^b), 3.78 (1H, ddd, J_{HH} = 3, 12, 14 Hz, H^{10}), 4.00 (1H, d, J_{HH} = 11 Hz, H^5), 4.42 (1H, br d, J_{HH} = 9 Hz, NH^a), 6.63 (2H, d, J_{HH} = 7 Hz, H^7), 6.68 (2H, d, J_{HH} = 7 Hz, H^8), 6.73−6.76 (1H, m), 6.90−6.92 (2H, m), 7.04 (2H, d, J_{HH} = 9 Hz), 7.12−7.13 (3H, m), 7.27 (2H, d J_{HH} = 9 Hz).

Cp*RhCl(4-FC$_6$H$_4$SO$_2$NCHPhCHPhNH$_2$) (2c). [Cp*RhCl$_2$]$_2$ (0.83 g, 1.35 mmol), 4-FC$_6$H$_4$SO$_2$DPEN (1.0 g, 2.7 mmol), and NEt_3 (0.75 mL,5.4 mmol) were reacted in CH_2Cl_2 (50 mL) to give **2c** (1.35 g, 78%). Crystals suitable for X-ray analysis were grown by slow diffusion of hexane into a concentrated solution of **2c** in CH_2Cl_2. ^{1}H NMR (500 MHz, $CDCl_3$, 300 K): δ 1.80 (15H, s, C_5Me_5), 3.54 (1H, br d, $J_{HH} \approx$ 10 Hz, NH^b), 3.70 (1H, ddd, J_{HH} = 2, 12, 14 Hz, H^{10}), 3.84 (1H, br apparent t, $J_{HH} \approx$ 11, 11 Hz, NH^a), 3.96 (1H, d, J_{HH} = 11 Hz, H^5), 6.62 (2H, d, J_{HH} = 9 Hz, H^7 or H^8), 6.65−6.68 (2H, m, H^7 or H^8), 6.78 (2H, apparent t, J_{HH} = 8, 8 Hz, H^2), 6.82−6.85 (3H, m, H^9 and H^{12}), 7.10 (3H, m, H^{13} and H^{14}), 7.40 (2H, dd, J_{HH} = 8 Hz, J_{HF} = 5 Hz, H^3). ^{13}C (125 MHz, CD_2Cl_2, 300 K): δ 9.96 (s, C_5Me_5), 69.85 (s, C^5), 71.87 (s, C^{10}), 94.92 (d, J_{RhC} = 8 Hz, C_5Me_5), 113.9 ($C^{2,d}$, J_{FC} = 22 Hz), 127.09 (s, C^9 or C^{12}), 127.55 (s, C^9 or C^{12}), 127.66 (s, C^7 or C^8), 128.79 (s, C^{13} or C^{14}), 128.96 (s, C^{13} or C^{14}), 129.32 (s, C^7 or C^8), 130.79 (d, J_{FC} = 6 Hz, C^3), 139.87 (s, C^5 or C^{10}), 139.94 (s, C^5 or C^{10}), 141.70 (s, C^4), 163.43 (d, J_{FC} = 250 Hz,C^1). ^{19}F NMR (480 MHz, CD_2Cl_2, 300 K): δ −112.76 (s). ^{1}H–^{15}N HMQC NMR (50.7 MHz, CD_2Cl_2, 300 K): δ −263.8 (d, J_{RhN} = 16 Hz, NH_2), −210.2 (d, J_{RhN} = 21 Hz, NTos). ^{1}H−^{103}Rh HMQC (22.18 MHz, $CDCl_3$, 300 K): δ 2036.5. MS (FAB, *m*/*z*): 643 ([$MH]^+$). IR (KBr/cm^{-1}): 3292 (ν_{NH}), 3234 (ν_{NH}). Anal. Calcd for $C_{30}H_{33}ClFN_2O_2RhS$: C, 56.04; H, 5.17, N, 4.36. Found: C, 55.70; H, 5.39; N 4.39.

^{1}H NMR (500 MHz, CD_3CN, 300 K): δ 1.80 (15H, s, C_5Me_5), 3.61 (1H, br apparent t, $J_{HH} \approx$ 11, 11 Hz, NH^b), 3.80 (1H, ddd, J_{HH} = 3, 12, 14 Hz, H^{10}), 3.94 (1H, d, J_{HH} = 11 Hz, H^5), 4.44 (1H, br d, $J_{HH} \approx$ 8 Hz, NH^a), 6.69 (2H, d, J_{HH} = 7 Hz), 6.75−6.79 (4H, m), 6.83−6.85 (1H, m), 6.89−6.91 (2H, m) 7.12−7.14 (3H, m), 7.44 (2H, dd J_{HH} = 9 Hz, J_{FH} = 5 Hz).

^{15}N-Labeled Cp*RhCl(TsNCHPhCHPhNH$_2$) (2a-^{15}N). [Cp*RhCl$_2$]$_2$ (36.0 mg, 58 μmol), TsDPEN (41.0 mg, 112 μmol), and NEt_3 (33 μL, 237 μmol) were reacted in CH_2Cl_2 (5 mL), to give ^{15}N-enriched **2a** (54 mg, 71%). ^{1}H NMR (500 MHz, $CDCl_3$, 300 K): δ 1.80 (15H, s, C_5Me_5), 2.21 (3H, s, Me), 3.48 (1H, dd, J_{NH} = 72 Hz, J_{HH} = 10 Hz), 3.70 (1H, ddd, J_{HH} = 14, 12, 3 Hz), 3.86 (1H, d of apparent t, J_{NH} = 82 Hz, J_{HH} = 11, 11 Hz), 3.96 (1H, d, J_{HH} =11 Hz), 6.63 (2H, d, J_{HH} = 7 Hz), 6.75 (2H, t, J_{HH} = 7 Hz), 6.80−6.85 (5H, m), 7.06−7.14 (3H, m), 7.28 (2H, d, J_{HH} = 7 Hz). ^{15}N{^{1}H} NMR (50.7 MHz, CD_2Cl_2, 300 K): δ −263.6 (d, J_{RhN} = 14 Hz, NH_2), −210.6 (d, J_{RhN} = 18 Hz, NTs). MS (FAB, *m*/*z*): 639 ([MH^+] ^{14}N/^{14}N isotopomer), 640 ([$MH]^+$ ^{14}N/^{15}N isotopomer), 641 ([$MH]^+$ ^{15}N/^{15}N isotopomer).

Synthesis of [Cp*Rh(CO)(CONTsCHPhCHPhNH$_2$)][Cl] (3a). **3a** was prepared by adding CO (3 atm) to an NMR tube fitted with a Young's tap containing a degassed solution of **2a** in dry CD_2Cl_2, CD_3OD, or a mixture of CD_2Cl_2/CD_3OD (1%). ^{1}H NMR (500 MHz, CD_2Cl_2, 300 K): δ 1.68 (s, 15H, C_5Me_5), 1.83 (s, 15H, C_5Me_5), 2.28 (s, 3H, Me), 2.31 (s, 3H, Me), 4.49−4.51 (m, 2H, CH), 5.04−5.09 (m, 2H, CH), 6.02 (d, J_{HH} = 6 Hz, 1H, NH), 6.07 (d, J_{HH} = 6 Hz, 1H, NH), 6.82−7.40 (m, 28H, aromatic), 7.56 (m, 1H, NH), 7.78 (d, J_{HH} = 8 Hz, 1H, NH). ^{13}C NMR (75 MHz, CD_2Cl_2, 300 K): δ 9.06 (s, C_5Me_5), 9.30 (s, C_5Me_5), 21.16 (s, Me), 60.72 (s, CH), 60.84 (s, CH), 63.55 (s, CH), 64.10 (s, CH), 106.24 (d, J_{RhC} = 5 Hz, C_5Me_5), 106.55 (d, J_{RhC} = 5 Hz, C_5Me_5), 124.86 (s), 126.90 (s), 127.26 (s), 127.59 (s), 127.66 (s), 127.78 (s), 127.83 (s), 128.44 (s), 128.68 (s), 129.10 (s), 129.32 (s), 137.30 (s), 137.46 (s), 137.95 (s), 138.24 (s), 138.36 (s), 138.43 (s), 142.77 (s), 142.98 (s), 181.58 (d, J_{RhC} = 27 Hz, NCO), 181.75 (d, J_{RhC} = 27 Hz, NCO), 188.08 (d, J_{RhC} = 77 Hz, CO), 188.14 (d, J_{RhC} = 77 Hz, CO). ^{13}C NMR (125 MHz, CD_2Cl_2, 300 K): δ 181.6 (d, J_{RhC} = 27 Hz, NCO), 181.7 (d, J_{RhC} = 27 Hz, NCO), 188.1 (d, J_{Rhc} = 77 Hz, CO), 188.2 (d, J_{Rhc} = 77 Hz, CO). MS (FAB, *m*/*z*): 603 ([M − 2CO]$^+$). IR (CH_2Cl_2/cm^{-1}): 2056 (ν_{CO}), 1600 (ν_{CO}).

[Cp*Rh(*t*BuNC)(TsNCHPhCHPhNH$_2$)][PF$_6$] (4a). 4a was prepared by addition of *t*BuNC (13 mg, 0.16 mmol) to a solution of **2a** (100 mg, 0.16 mmol) in CH_3OH (5 mL), stirring for 1 h, removing the solvent under reduced pressure, and extracting into toluene. The addition of KPF_6 (59 mg, 0.32 mmol) to the toluene solution resulted in the precipitation of a yellow solid. The yellow solid was extracted into THF, filtered, and crystallized from THF/hexane to give **4a** (102 mg, 76%) as yellow needles. ^{1}H NMR (500 MHz, CD_3CN, 300 K): δ 1.70 (s, 9H, *t*Bu), 1.91 (s, 15H, C_5Me_5), 2.15 (s, 3H, Me), 3.75 (ddd, J_{HH} = 3, 12, 14 Hz, 1H, H^{10}), 4.09 (br d, $J_{HH} \approx$ 11 Hz, 1H, NH^a), 4.15 (d, J_{HH} = 11 Hz, 1H, H^5), 4.29 (br apparent t, $J_{HH} \approx$ 11, 11 Hz, 1H, NH^b), 6.60 (d, J_{HH} = 7 Hz, 2H, Ph), 6.65 (t, J_{HH} = 8 Hz, 2 H, Ph), 6.74 (d, J_{HH} = 8 Hz, 2H, H^2), 6.74−6.76 (m, 1H, H^9, or H^{14}), 7.03−7.04 (m, 2H, Ph), 7.12 (d, J_{HH} = 8 Hz, 2H, H^3), 7.18 (m, 3H, Ph). ^{13}C NMR (125 MHz, CD_3CN, 300 K): δ 10.33 (s, C_5Me_5), 21.50 (s), 30.64 (s, CMe_3), 60.37 (s, CMe_3), 71.74 (s, C^{10}), 73.84 (s, C^5), 102.26 (d, J_{RhC} = 7 Hz, C_5Me_5), 127.60 (s, Ph), 128.52 (s, Ph), 128.77 (s, Ph), 129.03 (s, C^2), 129.33 (s, C^3), 129.62 (s, Ph), 130.00 (s, Ph), 134.8 (d, J_{RhC} = 69, CN), 139.69 (s, Ph), 140.11 (s, Ph), 141.40 (s, C^1 or C^4), 141.91 (s, C^1 or C^4). ^{31}P NMR (202 MHz, CD_3CN, 300 K): δ −144.61 (sept, J_{FP} = 702 Hz). MS (ESI, *m*/*z*): 686 ([M^+]). IR (KBr/cm^{-1}): 3336 (ν_{NH}), 3292 (ν_{NH}); 2212 (ν_{CN}). Anal. Calcd for $C_{36}H_{45}F_6N_3O_2PRhS$: C, 51.99; H, 5.42; N, 5.05. Found: C, 51.68; H, 5.48; N, 4.99.

[(Cp*Rh)$_2$(μ-H)(μ-Cl)(μ-HCO$_2$)][BPh$_4$] ([5a][BPh$_4$]). 2a (200 mg, 0.32 mmol) was dissolved in CH_3OH (10 mL) with the aid of sonication, and HCO_2H (150 mg, 3.26 mmol) was added via microsyringe. The solution turned from orange to red and was stirred for a further 15 min before stirring was stopped and $NaBPh_4$ (220 mg, 0.64 mmol) was added as a solid, and the flask was swirled to afford mixing, causing a red precipitate to settle from the solution upon standing. The solid was removed by filtration, dried under reduced pressure, and crystallized from acetone/Et_2O (1:1) at −20 °C to give **[5a][BPh$_4$]** as red crystals (121 mg, 43%). Crystals suitable for X-ray analysis were grown from a solution of **[5a][BPh$_4$]** in $(CH_3)_2CO$/Et_2O (1:1) at −20 °C. ^{1}H NMR (500 MHz, $(CD_3)_2CO$, 300 K): δ −8.59 (t, J_{RhH} = 27.4 Hz, 1H, Rh-*H*-Rh), 1.94 (s, 30H, C_5Me_5), 6.77 (t, J_{HH} = 7.2 Hz, 4H, BPh_4), 6.92 (t, J_{HH} = 7.5 Hz, 8H, BPh_4), 7.33−7.35 (m, 8H, BPh_4), 7.46 (t, J_{HH} = 3.5 Hz, 1H, HCO_2). ^{13}C NMR (125 MHz, $(CD_3)_2CO$, 300 K): δ 10.09 (s, C_5Me_5), 98.93−98.99 (m, C_5Me_5), 122.29 (s, BPh_4), 126.01−126.08 (q, J_{BC} = 3 Hz, BPh_4), 137.07−137.08 (m, BPh_4), 164.40−165.58 (q, J_{BC} = 49 Hz, BPh_4), 173.84 (s, HCO_2). IR (KBr/cm^{-1}): 1556 (ν_{CO}). MS (ESI, *m*/*z*): 557 ([$M]^+$). Anal. Calcd for $C_{45}H_{52}BClO_2Rh_2$: C, 61.63; H, 5.98. Found: C, 61.21; H, 6.12.

Transfer Hydrogenation of d_6-Acetone with d_{15}-NEt$_3$/Formic Acid Catalyzed by 2a. (*S,S*)-**2a** (4.4 mg, 6.8 μmol) was dissolved in CD_3CN; d_6-acetone (10 μL, 0.14 mmol) was added to the tube via microsyringe followed by d_{15}-NEt_3 (35 μL, 0.27 mmol). At each stage of addition, a ^{1}H NMR spectrum was recorded. The sample was cooled to 250 K, HCO_2H (26 μL, 0.680 mmol) was added to

the tube, and spectra were recorded every 10 min for 1 h. The experiment was repeated at 300 K.

Metathesis Reactions of 2a and 2c. Cp*RhCl(4-$RC_6H_4SO_2$NCHPhCHPhNH$_2$) was dissolved in the minimum volume of CH_3OH (often with the aid of sonication), the relevant reagent was added as a solid (LiBr, KI, AgOTf) or liquid (*t*BuNC), and the solution was stirred for 1 h or more. The solvent was removed under reduced pressure and the residue extracted into CH_3CN, filtered through Celite, and concentrated to dryness under vacuum. The product was recrystallized by layering a THF solution with hexane.

Synthesis of Cp*RhBr(TsNCHPhCHPhNH$_2$) (6a). 6a was prepared as described above from **2a** (150 mg, 0.23 mmol), LiBr (21 mg, 0.24 mmol), and CH_3OH (10 mL). After removal of CH_3CN the product was crystallized from THF/hexane to give **6a** (140 mg, 89%) as red crystals. Crystals suitable for X-ray analysis were grown by slow diffusion of hexane into a concentrated solution of **6a** in THF. ^{1}H NMR (500 MHz, CD_3CN, 300 K, numbering as in Figure 2): δ 1.82 (s, 15H, C_5Me_5), 2.19 (s, 3H, Me), 3.75 (br apparent t, $J_{HH} \approx 11$, 11 Hz, 1H, NH^a), 3.83 (ddd, $J_{HH} = 3$, 12, 14 Hz, 1H, H^{10}), 4.14 (d, $J_{HH} = 11$ Hz, 1H, H^5), 4.62 (br d, $J_{HH} \approx 10$ Hz, NH^b), 6.65−6.71 (m, 4H, Ph), 6.76−6.77 (m, 1H, Ph), 6.80 (d, $J_{HH} = 8$ Hz, 2H, H^3), 7.05 (m, 2H, Ph), 7.12−7.13 (m, 3H, Ph), 7.23 (d, $J_{HH} = 8$ Hz, 2H, H^2). ^{13}C NMR (125 MHz, CD_3CN, 300 K): δ 10.41 (s, C_5Me_5), 21.55 (s, Me), 70.39 (s, C^{10}), 72.55 (s, C^5), 95.96 (d, $J_{RhC} = 9$ Hz, C_5Me_5), 127.47 (s, Ph), 128.31 (s, Ph), 128.88 (s, C^2 and Ph), 129.13 (s, Ph), 129.20 (s, H^2), 129.48 (s, Ph), 130.34 (s, Ph), 140.52 (s, C^1), 140.96 (s, Ph), 141.08 (s, Ph), 143.07 (s, C^4). IR (KBr)/cm^{-1}): 3271 (ν_{NH}), 3210 (ν_{NH}). MS (FAB, *m*/*z*): 682 ([M$^+$] ^{79}Br isotopomer), 684 ([M$^+$] ^{81}Br isotopomer).

Cp*RhI(TsNCHPhCHPhNH$_2$) (7a). 7a was prepared as described above from **2a** (250 mg, 0.34 mmol) and KI (57 mg, 0.34 mmol) in CH_3OH (12 mL). The product was recrystallized from THF/hexane to give **7a** (174 mg, 70%) as dark red crystals. Crystals suitable for X-ray analysis were grown by slow evaporation of a solution of **7a** in CH_3OH. ^{1}H NMR (500 MHz, CD_3CN, 300 K): δ 1.92 (s, 15H, C_5Me_5), 2.21 (s, 3H, Me), 3.83 (m, 1H, H^a), 3.84 (m, 1H, H^{10}), 4.01 (d, $J_{HH} = 11$ Hz, 1H, H^5), 4.35 (br d, $J_{HH} \approx 9$ Hz, 1H, H^b), 6.66−6.69 (m, 4H, Ph), 6.74−6.76 (m, 1H, Ph), 6.80 (d, $J_{HH} = 8$ Hz, H^3), 6.92−6.94 (m, 2H, Ph), 7.12−7.13 (m, 3H, Ph), 7.21 (d, $J_{HH} = 8$ Hz, 2H, H^2). ^{13}C NMR (125 MHz, CD_3CN, 300 K): δ 11.11 (s, C_5Me_5), 21.46 (s, Me), 71.29 (s, C^{10}), 72.16 (s, C^5), 96.12 (d, $J_{RhC} = 8$ Hz, C_5Me_5), 127.37 (s, Ph), 128.06 (s, Ph), 128.67 (s, C^2), 128.87 (s, C^3), 129.06 (s, Ph), 129.51 (s, Ph), 130.58 (s, Ph), 140.19 (s, C^1), 140.33 (s, Ph), 141.22 (s, Ph), 144.46 (s, C^4). IR (KBr/cm^{-1}): 3278 (ν_{NH}), 3233 (ν_{NH}). MS (FAB, *m*/*z*): 731 ([MH]$^+$). Anal. Calcd for $C_{31}H_{36}IN_2O_2RhS$: C, 50.97; H, 4.97; N, 3.83. Found: C, 50.45; H, 5.03; N, 3.61.

[Cp*Rh(4-$FC_6H_4SO_2$NCHPhCHPhNH$_2$)][CF_3SO_3], [8c][OTf] and [8c-H_2O][OTf]. [8c][OTf] was prepared as described above from **2c** (500 mg, 0.78 mmol), $AgCF_3SO_3$ (200 mg, 0.78 mmol), and CH_3OH (40 mL). The product mixture was filtered through Celite before the solvent was removed under vacuum. Compound **[8c][OTf]** (470 mg, 80%) was obtained as a purple powder. Crystals suitable for X-ray analysis were grown by slow diffusion of hexane into a concentrated solution of **[8c][OTf]** in CH_3OH/toluene (1:1) but proved to be **[8c-H_2O][OTf]**. ^{1}H NMR (500 MHz, CD_3CN, 300 K): δ 1.83 (s, 15H, C_5Me_5), 3.75 (ddd, $J_{HH} = 3$, 12, 14 Hz, 1H, H^{10}), 3.95 (apparent t, 11 Hz,1H NH^b), 4.15 (d, 11 Hz, 1H, H^5), 4.50 (d, $J_{HH} = 10$ Hz, 1H, NH^a), 6.63−6.68 (m, 4H, Ph), 6.70 (apparent t, $J_{HH} = 8$ Hz, $J_{FH} = 8$ Hz, 2H, H^2), 6.76−6.79 (m, 1H, Ph), 7.06−7.08 (m, 2H, Ph), 7.16−7.17 (m, 3H, Ph), 7.31 (dd, $J_{HH} = 11$ Hz, $J_{FH} = 5$ Hz, 2H, H^3). ^{13}C NMR (125 MHz, CD_3CN, 300 K): δ 9.71 (s, C_5Me_5), 70.65 (s, C^{10}), 72.64 (s, C^5), 98.08 (d, $J_{RhC} = 8$ Hz, C_5Me_5), 115.10 (d, $J_{FC} = 22$ Hz, C^2), 122.09 (q, $J_{FC} = 316$ Hz, CF_3), 127.49 (s, Ph), 128.23 (s, Ph), 129.09 (s, Ph), 129.13 (s, Ph), 129.81 (s, Ph), 130.85 (d, $J_{FC} = 10$ Hz, C^3), 139.59 (s, Ph ipso), 139.94 (s, Ph ipso), 142.09 (d, $J_{FC} = 4$ Hz, C^4), 163.84 (d, $J_{FC} = 243$ Hz, C^1). ^{19}F NMR (470 MHz, CD_3CN, 300 K): δ −79.2 (s, 3F, CF_3), −113.0 (s, 1F, FC_6H_4). MS (ESI, *m*/*z*): 607 ([M]$^+$). IR (KBr/cm^{-1}): 3278 (ν_{NH}), 3246 (ν_{NH}). Anal. Calcd for **[8c-H_2O][OTf]**, $C_{31}H_{35}F_4N_2O_6RhS_2$: C, 48.07; H, 4.55; N, 3.62. Found: C, 47.89; H, 4.51; N, 3.65.

[Cp*Rh(*t*BuNC)(4-$FC_6H_4SO_2$NCHPhCHPhNH$_2$)][CF_3SO_3] (4c). 4c was prepared from **8c** by adding *t*BuNC (11 mg, 0.13 mmol) to a solution of **8c** (100 mg, 0.13 mmol) in CH_3OH (3 mL), filtering, and removing the solvent under vacuum, to give **4c** (46 mg, 55%) as a yellow powder. ^{1}H NMR (500 MHz, CD_3CN, 300 K): δ 1.70 (s, 9H, CMe_3), 1.91 (s, 15H, C_5Me_5), 3.75 (ddd, $J_{HH} = 3$, 12, 14 Hz, 1H, H^{10}), 4.12−4.18 (m, 1H, NH^a), 4.15 (d, $J_{HH} = 11$ Hz, 1H, H^5), 4.44 (br apparent t, $J_{HH} \approx 12$, 12 Hz, 1H, nH^b), 6.63−6.68 (m, 4H, Ph), 6.70 (dd, $J_{HH} = 8$ Hz, $J_{FH} = 8$ Hz, 2H, H^2), 6.76−6.79 (m, 1H, Ph), 7.04−7.07 (m, 2H, Ph), 7.17−7.18 (m, 3H, Ph), 7.26−7.28 (dd, $J_{FH} = 5$ Hz, $J_{HH} = 9$ Hz, 2H, H^3). ^{13}C NMR (125 MHz, CD_3CN, 300 K): δ 10.39 (s, C_5Me_5), 30.68 (s, CMe_3), 60.62 (s, CMe_3), 71.80 (s, C^{10}), 73.76 (s, C^5), 102.26 (d, $J_{RhC} = 7$ Hz, C_5Me_5), 115.62 (d, $J_{FC} = 23$ Hz, C^2), 122.81 (q, $J_{FC} = 335$ Hz, CF_3), 128.01 (s, Ph), 128.75 (s, Ph), 129.14 (s, Ph), 129.69 (s, Ph), 130.20 (s, Ph), 131.44 (d, $J_{FC} = 10$ Hz, C^3), 139.61 (s, Ph), 140.09 (s, Ph), 141.37 (d, $J_{FC} = 4$ Hz, C^4), 164.0 (d, $J_{FC} = 243$ Hz, C^1). ^{19}F NMR (470 MHz, CD_3CN, 300 K): δ −79.23 (s, 3F, CF_3), −112.63 (s, 1F, FC_6H_4). MS (ESI, *m*/*z*): 690 ([M]$^+$).

X-ray Crystallography. X-ray data were collected on a Bruker SMART Apex X-ray diffractometer for $\theta > 1.72°$ up to $\theta < 28.1-29.99°$. The crystals were cooled to 110 K using an Oxford Cryosystems Cryostream. Diffractometer control, data collection, and initial unit cell determination were performed using SMART (v5.625 Bruker-AXS). Frame integration and unit-cell refinement were carried out with SAINT+ (v6.22, Bruker AXS). Absorption corrections were applied by SADABS (v2.03, Sheldrick). The structures were solved by direct methods using SHELXS-97 and refined by full-matrix least-squares using SHELXL-97.[63,64] Hydrogen atoms bound to carbon were placed using a riding model and included in the refinement at calculated positions. Hydrogen atoms attached to nitrogen in **2c**, **6a**, and **7a** were located on difference maps after all non-hydrogen atoms had been located and were refined isotropically (**2c**, **7a**). Crystal data for complexes **2c**, **[5a][BPh_4]·OEt_2**, **6a**, **7a**, and **8c-H_2O** are shown in Table 2.

Acknowledgment. We acknowledge the support of EPSRC and NPIL Ltd. We also appreciated discussions with Matthew Stirling, George Hodges, Anthony Haynes, and Richard Douthwaite. We thank David Taylor for recording the rhodium NMR spectra, and Richard Lindup for assistance with preparing the manuscript. We thank the reviewer for helpful criticism of the manuscript.

Supporting Information Available: Cif files for **2c**, **[5a][BPh_4]·OEt_2**, **6a**, **7a**, and **8c·H_2O**. This material is available free of charge via the Internet at http://pubs.acs.org.

OM8009969

(63) Sheldrick, G. M. *SHELXS-97, a program for crystal structure solution*; Göttingen University: Germany, 1997.

(64) Sheldrick, G. M. *SHELXL-97, a program for crystal structure determination*; Göttingen University: Germany, 1997.